**Supplementary Material 1:**

## Materials and Methods

### Mice

The targeting vector *Inpp5k*$^{tm1a(EUCOMM)Wtsi}$/PRPGS00065_A_A10 (Figure S1) was purchased from EuMMCR/EUCOMM and electroporated into C57BL/6 ES cells by Cyagen Biosciences, Inc. Correctly targeted ES cell clones were electroporated with the PGK-FLP-obpA plasmid to delete the LacZ-Neo cassette, resulting in *Inpp5K*$^{flox/+}$ ES cells. *Inpp5K*$^{flox/+}$ mice, where exons 2 and 3 of the *Inpp5K* gene are flanked by LoxP sites, were obtained by Cyagen Biosciences after *Inpp5K*$^{flox/+}$ ES cells injection in blastocysts. These mice crossed with *Vav1*-iCre (B6.Cg-Commd10Tg(Vav1-icre)A2Kio/J), mb1-Cre (C(Cg)-*Cd79atm1(cre)Reth*/EhobJ) or CD4-Cre (B6.Cg-Tg(Cd4-cre)1Cwi/BfluJ) mice. All mice were housed in an animal facility with a 12 h light/12 h dark cycle and had free access to food and water throughout the study period. All mouse studies were authorized by the Animal Care Use and Review Committee of the University of Liege.

### Reagents and antibodies

BV711 anti-mouse CD45R/B220 (#563892), BUV737 anti-mouse CD24/HAS (#565308), APC anti-mouse IgM (#562032), PE-CF594 anti-AKT$^{pS473}$ mAb (#562465), BV421 anti-mouse LY-51/BP1 (#740013), PE anti-mouse EBF1 (#565494), PE anti-mouse CD8a (#553032) and FITC anti-mouse CD4 (#553046) antibodies were purchased from BD Biosciences. APC rat anti-mouse CD43 (#143207), BV 421™ anti-mouse CD19 (#115538), AF 647 anti-PAX5 (#649704), PE anti-STAT5$^{pY694}$ (#699605), AF 647 anti-mouse CD3ε (#100324), biotin anti-mouse CD127/IL7Rα (#135006), PE anti-mouse

CD132/common γ chain (#132305), purified anti-mouse CD127/IL7Rα (#135002), FITC anti-human CD3 Antibody (317306), AF 647 anti-human CD4 Antibody (300523), PE anti-human CD8 Antibody (344705), BV 421 anti-human CD19 Antibody (363017), and APC anti-human CD20 Antibody (302309) antibodies were purchased from Biolegend. Anti-JAK1$^{pY1022}$ (#STJ90314), anti-JAK3$^{pY980/981}$ (#STJ196341), and anti-IL7Rα$^{pY449}$ (#STJ90721) antibodies were purchased from St-John's laboratory. AF 488 Cholera Toxin Subunit B (CtxB, #C34775), AF 546 cross-adsorbed goat anti-rat IgG (H+L) (#A-11081), AF 546 cross-adsorbed goat anti-rabbit IgG (H+L) (#A-11010), AF 488 highly cross-adsorbed goat anti-rabbit IgG (H+L) (#A-11034), TRITC cross-adsorbed goat anti-rat IgG (H+L) (#A18876) and AF 647 highly cross-adsorbed goat anti-rabbit IgG (H+L) (#A-21245) secondary antibodies, as well as JAK3 polyclonal antibody (7HCLC) (#711602) and monoclonal rabbit IgG anti-mouse CD132/γc antibodies (# MA5-29720) were purchased from Invitrogen. Anti-PtdIns(4,5)P2 biotin (#117Z B045) antibody was purchased from Tebu-Bio. Human/mouse/rat JAK1 antibody (#MAB4260) was purchased from RD System. AF 488 α-Tubulin (B-7) (#sc-5286) antibody was purchased from Santa Cruz Biotechnology. Clean-Blot™ IP Detection Reagent (HRP) (#21230) and DiO'/DiOC18(3) (3,3'-Dioctadecyloxacarbocyanine Perchlorate) (#D275) products were purchased from Thermofisher. β-Actin (13E5) rabbit mAb (#4970S) was purchased from CST. CD127/IL7R polyclonal antibody (#17626-1-AP) and human INPP5K Polyclonal antibody (15098-1-AP) were purchased from Proteintech. PE anti-mouse CD43 (leukosialin) (#120431) antibody was purchased from eBioscience. Rabbit anti-mouse INPP5K antibody was produced by Eurogentec and peptide affinity-purified in the Laboratory of Functional Genetics.

**Cell isolation**

Bone marrow was taken from femurs and tibias of 8- to 16-week-old mice. Tibias and femurs were first flushed with PBS/10mM EDTA + 2% FBS, filtrated on a 50µm membrane and centrifuged 5min at 350g. Then, pellet was resuspended in 5 ml of red blood lysis buffer (0,414g NH4Cl; 50mg KHCO3; EDTA 1mM pH8) 10min at RT. Lysis reaction was stopped by adding 10ml of PBS/10mM EDTA + 2% FBS and the resuspended solution was centrifuged 5min at 350g. Spleen was taken from 8- to 16-week-old mice and pressed in a 6 wells plate containing 2ml of red blood lysis buffer, 3 more ml were added and then incubated 10min at RT. Lysis was stopped with 10ml of PBS/10mM EDTA + 2% FBS and the solution was filtered on a 50µm membrane and then centrifuged 5min at 350g. Cardiac punction was performed on 8- to 12- week-old mice to collect blood in EDTA tube. Blood was then suspended in 10ml of red blood lysis buffer for 5min at RT and then centrifuged 5min at 350g. This step was realized two or three times. Pellets from bone marrow, spleen and blood cells were resuspended in 1ml of PBS/10mM EDTA + 2% FBS and alive cells were counted on a Neubauer counting chamber (Hirschmann # 8100103) with Trypan blue (Thermoscientific # SV30084.01).

**Hematology analyzer**

Blood cells were quantified with a Cell Dyn 3500 analyzer (Abott Diagnostic).

**$D_H$-$J_H$, $V_H$J558-$D_HJ_H$ and $V_H$J7183-$D_HJ_H$ recombination analysis**

Bone marrow B cells and neutrophils were purified with Mouse CD45R (B220) MicroBeads (#130-049-501) and Mouse Neutrophil Isolation Kit (#130-097-658) from Miltenyi Biotec, respectively. Genomic DNA was prepared for PCR by lysing bone marrow cells ($10^6$) with 350µl of TNES (400mM $NaCl^+$ 100mM EDTA pH 8-8,5 +0,6% SDS) + 0,2% proteinase K (Thermofisher Scientific #4333793) at 55°C during 3h. Vortexing was performed each 30min. NaCl 6M (100µl) was added and DNA containing

solution was centrifuged at 140000g during 10min. EtOH 100% (300 µl) was added to the supernatant. This solution was centrifuged at 14000g during 10min after 4 up and down mixing. Supernatant was removed, 300µl of EtOH 70% was added and centrifugation was performed at 14000g during 10min. Supernatant was removed and pellet was dried during 30min. Pellet was dissolved in 100µl of Tris-HCl pH 7,5-8,5 at 55°C during 1h. DNA was quantified with Thermo Scientific™ Spectrophotomètres NanoDrop™ 2000 / 2000c. PCR reaction (10µl) was prepared with GoTaq® G2 Hot Start Taq Polymerase kit (Promega # M7405): 1µl DNA template (100ng)+ 3,2µl $dH_20$ 1µl primer + 2µl buffer + 1µl MgCl2+ 0,8µl dNTP (Applied Biosystems #362275). The following primers, $J_H3$ (5'-*GTCTAGATTCTCACAAGAGTCCGATAGACCCTGG-3'*), DH (5'-*CGAATTCGATTTTTGTCAAGGGATCTACTACTGTG-3'*), $V_H558$ (5'-*CGAGCTCTCCAGCACAGCCTACATGCAGCTCAAC-3'*), VH7183 (5'-*CGGTACCAAGAACAACCTGTTCCTGCAAATGACC-3'*) were used to amplified recombined segments: 94°C-2min; (94°C - 1min; 60°C - 1min; 72°C - 1min45sec) X35; 72°C -10min. PCR products were charged on 1% gel and $D_H$-$J_H$, $V_H558$-$D_HJ_H$ and $V_H7183$-$D_HJ_H$ amplicons were detected at 1033, 716 and 333 bp, respectively.

**Blood immunoglobulins quantification**

Cardiac punction was performed on 8- to 12- week-old mice and blood was incubated at RT during at least 30 min and then centrifuged 5 min at 350g. The supernatant was removed in another tube. This step was repeated at least 2 times. Serum levels of IgG, IgM and IgA were determined by ELISA. Briefly, for VAV-CRE and control mice, plates were coated with goat anti-mouse IgG, goat anti-mouse IgM or goat anti-mouse IgA specific antibodies and the assays were developed with the respective alkaline phosphatase-conjugated goat anti-mouse isotype specific antibodies (all from Sigma).

Results were expressed in µg/ml for IgG and IgM or ng/ml for IgA antibodies in reference to a standard curve obtained with a mouse reference serum (ICN Biomedicals Inc.). For MB1-CRE and control mice, blood immunoglobulins quantification was determined with IgM Mouse Uncoated ELISA Kit (Plates #88-50470) and IgG (Total) Mouse Uncoated ELISA Kit (Plates # 88-50400-86), both purchased from Invitrogen. Absorbance analysis was performed by Tecan Infinite 200 Pro from LabX.

**Cell phenotyping, protein expression, Interleukin-7 (IL7) stimulation and Facs analysis**

For phenotyping, cells isolated from bone marrow, spleen and blood were diluted to $10^6$ cells/ml and then blocked with 100µl of PBS/10mM EDTA + FBS 5% + 2,5 ng/ml purified rat anti-mouse CD16/CD32 (BD Biosciences #553141) 20min at 4°C. Cells were then centrifuged 5min at 350g. Blood cells were stained with CD3ε, CD4, CD8 and CD19, splenic cells with CD19 and bone marrow cells with B220, CD43, CD24, BP-1, IgM and IgD for 30min at 4°C. Each mix was supplemented by 1/1000 Fixable Viability Dye eFluor™ 780 (eBioscience # 65-0865-14). For protein expression analysis, cells isolated from bone marrow were diluted to $5x10^6$ cells/ml and then blocked with 100µl of PBS/10mM EDTA + FBS 5% + 2,5 ng/ml purified rat anti-mouse CD16/CD32 (BD Biosciences #553141) for 20min at 4°C. Cells were centrifuged 5min at 350g and stained with B220, CD43, CD24, BP-1 antibodies and Fixable Viability Dye eFluor™ 780 in PBS/10mM EDTA + FBS 5% solution for 30min at 4°C. Stained cells were washed 2 times in PBS/10mM EDTA +FBS 2% for 5min at 350g, and then fixed with PAF 2% (Sigma Aldrich #HT501128) for 20min at 4°C. Cells were plasma and nuclear membranes-permeabilized with Foxp3/Transcription Factor Staining Buffer Set (eBioscience #00-5523-00) for 30min at 4°C. Cells were washed 2 times in PBS/10mM

EDTA +FBS 2% and stained 50min at RT with Alexa Fluor® 647 anti-PAX5 and PE anti-mouse EBF1 antibodies diluted in 100µl of PBS/EDTA+FBS 2% solution.

For *ex-vivo* IL-7 stimulation analysis, cells isolated from bone marrow were diluted to $5x10^6$ cells/ml and then blocked with 100µl of PBS/10mM EDTA + FBS 5% + 2,5 ng/ml purified rat anti-mouse CD16/CD32 (BD Biosciences #553141) for 20min at 4°C. Cells were centrifuged 5min at 350g, stained with B220, CD43, CD24, BP-1 antibodies and Fixable Viability Dye eFluor™ 780 in PBS/10mM EDTA + FBS 5% solution for 30min at 4°C and washed 2 times in PBS/10mM EDTA +FBS 2%. Mouse IL-7 Recombinant Protein (Invitrogen # RP-8664) (2ng/ml) was added to cells at 37°C for 0 (without IL-7), 2 and 10min. The activation was stopped by fixating cells with 2% PAF (Sigma Aldrich # HT501128) 15min at 4°C. Cells were washed 2 times in PBS/10mM EDTA +FBS 2%. Cells were plasma membrane-permeabilized with Intracellular Fixation & Permeabilization Buffer Set (eBioscience # 88-8824-00). Cells were stained with PE-CF594 mouse anti-AKT$^{pS473}$, PE anti-STAT5$^{pY694}$, anti-JAK1$^{pY1022}$ and anti-JAK3$^{pY980/981}$ antibodies diluted in permeabilization buffer for 50min at RT and washed 2 times in PBS/10mM EDTA +FBS 2%. Cells were stained with PE-labeled F(ab')2-goat anti-rabbit IgG (H+L) secondary antibody (Invitrogen #A10542) for 15min at RT. BD FacsFortessa was used for cell phenotyping. Mean fluorescence intensity (MFI) of specific markers was quantified on B cell subpopulations using FlowJo. Results were analyzed using FlowJo (Tree Star, Ashland, USA).

**Immunofluorescence, FRET and Airyscan microscopy analysis**

Bone marrow cells were isolated and total B cells were purified with mouse CD45R (B220) MicroBeads (#130-049-501). Purified cells were stained with BV711 anti-mouse CD45R/B220, Fixable Viability Dye eFluor™ 780 and APC rat anti-mouse CD43 or PE

anti-mouse CD43 antibodies diluted in 100µl of PBS/10mM EDTA + FBS 5%. FSC-W and FSC-A discrimination was used to exclude doublet cells, and Fixable Viability Dye eFluor™ 780 was used to discriminate between dead and living cells. B cells precursors were sorted as $B220^{+}CD43^{+}$ cells using BD FACSAria III 4L sorter. Nunc™ Lab-Tek™ II Chamber Slide™ System (Thermo Scientific # 154534PK) was coated with Poly-D-lysine hydrobromide (Sigma-Aldrich #P7280) at least 2h at RT. Sorted $B220^{+}CD43^{+}$ cells (50µl containing 2-4x$10^{5}$ cells) were fixed on slide for 1h at RT. Mouse IL-7 Recombinant Protein (Invitrogen # RP-8664) (2ng/ml) was added to fixed cells for 0 (without IL-7), 2 and 10 min at 37°C. For $GM1^{+}$ microdomains detection, activation was stopped by fixating cells with 2% PAF (Sigma Aldrich # HT501128) for 15min at 4°C and cells were incubated with AF 488 Cholera Toxin Subunit B (CtxB) overnight at 4°C. $GM1^{+}$ microdomains were defined according to a florescence volume threshold. This volume threshold (0,002µ$m^{3}$) was experimentally defined using Imaris software in order to exclude background and non-specific fluorescence. For immunofluorescence, activation was stopped by fixating cells with 2% PAF (Sigma Aldrich # HT501128) for 15min at 4°C (for IL7Rα, INPP5K and PtdIns(4,5)P2 staining) and with MetOH 100% at -20°C for 20min (for α-Tubulin and β-Actin staining). Cells were washed 2 times in PBS/10mM EDTA +FBS 2%, blocked and permeabilized with a solution containing PIPES 0,65% + NaCl 0,8% + KCl 0,02% +saponin 0,5% + goat serum 10% for 45min at 4°C. Cells were stained with INPP5K, IL7Rα, PtdIns(4,5)P2, α-Tubulin and β-Actin antibodies diluted in PIPES 0,65% + NaCl 0,8% + KCl 0,02% +saponin 0,1% + goat serum 10% solution overnight at 4°C. Cells were washed 3 times in PBS solution and then incubated with secondary antibodies for 2h at 4°C. Cells were washed once in PBS, incubated for 10min with DAPI 10mM 1/1000 (Thermofisher # D1306) and washed 3 times with $dH_20$. Slide chambers were mounted

using ProLong (Invitrogen# P36970). Zeiss LSM880 Airyscan/SIM was used for Z-stacks images acquisition. Orthogonal reconstructions of the Z-stacks images were obtained with Zen blue and Zen black edition software. For FRET, cell activation was stopped by fixating cells with 2% PAF (Sigma Aldrich # HT501128) for 15min at 4°C and were washed 2 times in PBS/10mM EDTA +FBS 2%. For non-permeabilized condition, cells were blocked in PBS+EDTA 10mM +5% FBS and stained with 2,5µg of monoclonal rat IgG2a,κ anti-mouse IL7Rα (Biolegend # 135002 immunogen IL7Ra-IgG1 fusion protein), 5µg of monoclonal rabbit IgG anti-mouse CD132/γc antibodies (Invitrogen # MA5-29720 immunogen peptide aa 1-263) or 5µg of DiO' in PBS + 10mM EDTA +2%FBS overnight at 4°C. For intracellular staining, cells were blocked and plasma membrane permeabilized with a solution containing PIPES 0,65% + NaCl 0,8% + KCl 0,02% +saponin 0,5% + goat serum 10% for 20min at 4°C and stained with 5µg of monoclonal rat IgG2B anti-mouse/human JAK1 (RD systems #MAB4260 immunogen peptide aa 32-286), 2,5 µg of polyclonal rabbit IgG anti-human JAK3 (Invitrogen #711602 imunogen peptide aa 811-1124) or 5µg of polyclonal rabbit IgG anti-IL7Rα$^{pY449}$ (ST-Johns laboratory # STJ90721 binds to endogenous IL7Ra at the amino acid region 380-460 only when phosphorylated at Y449) antibodies diluted in PIPES 0,65% + NaCl 0,8% + KCl 0,02% +saponin 0,1% + goat serum 10% solution overnight at 4°C. For both condition, cells were washed 3 times in PBS and then incubated with AF546 cross-adsorbed goat anti-rat IgG (H+L) (against anti- IL7Ra/JAK1 antibodies) and AF488 highly cross-adsorbed goat anti-rabbit IgG (H+L) (against anti-CD132/JAK3 antibodies) secondary antibodies for 2h at 4°C. Cells were washed once in PBS, incubated 10min with DAPI 10mM 1/1000 (Thermofisher # D1306) and washed 3 times with $dH_20$. Slide chambers were mounted using ProLong (Invitrogen# P36970). FRET efficiency was obtained according to validated calculation that remove

fluorescence background (Guala et al., 2018). In analysis of indirect FRET, compensation for spectral spillover between donor and acceptor channels need to be performed. To this aim, each time, controls conditions were used: Cells probed with donor alone (AF488), with acceptor alone (AF546) and with both (AF488 +AF546).

- Donor alone (AF488)

B = (IDA') / (IDD)

IDA'= Fluorescence intensity from $\lambda_{\text{donor excitation}}$ and $\lambda_{\text{acceptor emisson}}$

IDD= Fluorescence intensity from $\lambda_{\text{donor excitation}}$ and $\lambda_{\text{donor emisson}}$

Compensation for donor probe (AF488) was established by illuminating the donor probe only sample with the donor excitation wavelength and measuring the background corrected mean intensities within a cell in both donor (IDD) and acceptor (IDA') channels. DIO' and AF488 highly cross-adsorbed goat anti-rabbit IgG (H+L) secondary antibody was excited with 488 nm laser line (Donor alone) and visualized using the bandpass 500 - 545 +LP 575 Airyscan filter (IDD) or visualized using the 595/40 bandpass + LP 655 Airyscan filter (IDA').

- Acceptor alone (AF546)

D = (IDA) / (IAA)

IDA= Fluorescence intensity from $\lambda_{\text{donor excitation}}$ and $\lambda_{\text{acceptor emission}}$

IAA= Fluorescence intensity from $\lambda_{\text{acceptor excitation}}$ and $\lambda_{\text{acceptor emission}}$

Compensation for direct excitation of the acceptor was established using the acceptor probe only (AF546) sample by measuring the background corrected mean intensities within a cell in the acceptor channel using donor excitation wavelength (IDA) and acceptor excitation wavelength (IAA). AF546 cross-adsorbed goat anti-rat IgG (H+L) was excited

with 561nm laser line (Acceptor alone) and visualized using the bandpass 500 - 545 +LP 575 Airyscan filter (IDA) or using the 595/40 bandpass + LP 655 Airyscan filter (IAA).

- Donor and Acceptor (AF488 +AF546)

ID= Fluorescence intensity from $\lambda_{\text{donor excitation}}$ and $\lambda_{\text{donor emission}}$

IA= Fluorescence intensity from $\lambda_{\text{donor excitation}}$ and $\lambda_{\text{acceptor emission}}$

IA'= Fluorescence intensity from $\lambda_{\text{acceptor excitation}}$ and $\lambda_{\text{acceptor emission}}$

FRET_corr = IA - B*ID -D*IA'

FRET_efficiency = FRET_corr /ID

The samples with both donor probe (AF488) and acceptor probe (AF546) were used to measure FRET. The background corrected intensity in donor (ID) and acceptor channels (IA) were recorded using donor excitation wavelength followed by recording the intensity in the acceptor channel (IA') using acceptor excitation wavelength. The compensation factors B and D, were used to calculate on a pixel-by-pixel basis the corrected FRET intensity (FRETcorr) and the FRET ratio (FRET efficiency) which was reported as a mean value for each analyzed cell and experimental group. For FRET emission (Donor + Acceptor), only visualization using the 595/40 bandpass + LP 655 Airyscan filter was performed after 561 nm laser line excitation (IA'), but after 488 nm laser line excitation, visualization was performed using the bandpass 500 - 545 +LP 575 Airyscan filter (ID) and using the 595/40 bandpass + LP 655 Airyscan filter (IA).

For FRET positive control, as previously described, cells were blocked, plasma membrane permeabilized, incubated with 5µg of monoclonal rat IgG2B anti-mouse/human JAK1 (RD systems #MAB4260 immunogen peptide aa 32-286) and then incubated with AF546 cross-adsorbed goat anti-rat IgG (H+L) and AF488 cross-adsorbed goat anti-rat IgG (H+L). FRET efficiency from positive control is defined as higher limit detection. For FRET

negative control, cells were first, as previously described, blocked, plasma membrane permeabilized, incubated with 5µg of monoclonal rat IgG2B anti-mouse/human JAK1 (RD systems #MAB4260 immunogen peptide aa 32-286) and incubated a second time with AF546 cross-adsorbed goat anti-rat IgG (H+L) Secondly, cells were blocked and nuclear-permeabilized with PBS+5%goat serum +0,3% tritonX100, incubated with monoclonal rabbit IgG anti-mouse PAX5 antibody (CST #12709 immunogen carboxy terminal part) 1/100 and then with AF488 cross-adsorbed goat anti-rabbit IgG (H+L). Antibody dilution solution for nuclear staining used contain PBS +1% BSA +0,1% triton X100. FRET efficiency from negative control is defined as lower limit detection.

Zeiss LSM880 Airyscan/SIM was used for Snap images acquisition. Fiji was used for script generation, FRET efficiency calculation and image production. The script and methods of statistical analysis are available with this link:

https://github.com/Alexh3g0/Indirect_FRET

**Tryptophan fluorescence emission spectrum (TFES) assay**

Bicelles (q=0.8) were prepared by mixing the long-chain phospholipids POPG (1-Palmitoyl-2-oleoyl-phosphatidylglycerol) or POPC (1-palmitoyl-2-oleoyl-phosphatidylcholine) with the short-chain phospholipid DHPC (dihexanoyl-phosphatidylcholine) at a ratio of 0.8:1 (POPG/POPC:DHPC) in 10 mM Tris-HCl buffer (pH 7.4). The mixture was subjected to several freeze-thaw cycles with vortexing until the lipids were fully dissolved. To measure the TFES of wild type and mutated IL7Rα juxtamembrane cytoplasmic 45 amino acids peptides, 2–4 µM peptide and 0–200 µM POPG, POPC or PtdIns(4,5)P2/POPC lipids bicelles were mixed and incubated for 20 min at RT. A Varian Cary Eclipse machine was used with the excitation wavelength 290

nm and emission wavelength 300–400 nm. The sample buffer was 10 mM Tris-HCl, pH 7.4.

**BaF3 and DND-41 cell culture, transduction and analysis:**

The mouse pro-B Ba/F3 cell line transduced with pMIG expressing the human mutated p.Thr244_Ile245 insCysProThr IL7Rα (CA-IL7Rα) chain and the human T-ALL DND-41 cell line carrying the constitutively activated p.Leu242_Leu243 insLeuSerArgCys IL7Rα chain insertion mutation (among other mutations in NOTCH1, EGFR, NRAS, MAP2K4, RB1 or TP53 genes (https://www.cellosaurus.org/CVCL_2022)) were maintained in culture medium (RPMI-1640 supplemented with 10% FBS (Thermofisher #25030081), penicillin/streptomycin 50U/ml (Thermofischer #15070063), amphotericin B 0,25µg/ml (Thermofischer #15290026) at 37°C 5% CO2. CA-IL7Rα BaF3 cells were transduced in the GIGA-Viral Vectors platform with lentiviral particles expressing one of these 5 shRNAs directed against the mouse *Inpp5k* mRNA: 1 (ACTACGTCAGCATCATCAATT), 2 (ACGTCTGCCTGAAGCTTTATG), 3 (GCCCAGATGGAAGTGAATGA), 4 (CCCAGATGGAAGTGAATGAAT), 5 (CCTGAAGCTTTATGGCTACTA), or a control shRNA (mock, CCTAAGGTTAAGTCGCCCTCG) in pLV [shRNA]-TagBFP2-U6, obtained from VectorBuilder GmbH, Germany. All described experiments on CA-IL7Rα BaF3 cells were performed with the most efficient shINPP5K, shINPP5K 5. DND-41 cells were transduced with lentiviral particles expressing one of these 5 shRNAs directed against the human *INPP5K* mRNA: 1 (TCTGGAATTAGCCGCTTAAAT), 2 (TATCAGCATTTGCCCTATATC), 3 (CTTTGTTCGGGAATCCATTAA), 4 (CCTGAAGCTTTATGGCTACTA), 5 (CGGAACCTCAATCTTGACATA), or a control shRNA (mock, CCTAAGGTTAAGTCGCCCTCG) in pLV [shRNA]-TagBFP2-U6, obtained from VectorBuilder GmbH, Germany. All described experiments on DND-41

cells were performed with the most efficient shINPP5K, shINPP5K 5. INPP5K, p-STAT5$^{Y694}$ and PtdIns(4,5)P2 signals were analyzed by flow cytometry on plasma membrane-permeabilized cells as described above. A similar flow cytometry procedure was used for BCL-2 and BCL-XL signals. Levels of AKT, p-AKT, S6, p-S6, STAT5, p-STAT5A/B$^{Y694/699}$, ERK1/2, p-ERK1/2 and c-MYC were analyzed by Western blotting as described (Almeida, A.R.M., et al., 2021). CA-IL7Rα Ba/F3 cell counts were performed as described (Zenatti, P. P., et al., 2011). Total cell counts were calculated by trypan blue exclusion using a hemocytometer. Indirect FRET analysis between the excited donor DiO' membrane fluorophore and the acceptor fluorophore-labeled secondary antibody which recognizes the primary antibody directed against p-IL7Rα$^{Y449}$ was performed as described above.

**Supplementary Material 2:**

**Lack of INPP5K induces severe lymphopenia and hypoglobulinemia, and impairs normal B cell differentiation and maturation**

In order to study the effects of the *Inpp5k* gene inactivation on mouse hematopoietic cells differentiation and to define the functions of the 5-phosphatase in these cells, a mutant *Inpp5k*$^{flox/+}$ mouse was generated in which two intronic LoxP sites were introduced upstream of exon 2 and downstream of exon 3 in the *Inpp5k* gene (Figure S1A). Crossing *Inpp5k*$^{flox/+}$ mutants with *PGK-Cre* mice generated *Inpp5k*$^{\Delta/+}$ mice with a full body heterozygous deletion of exons 2 and 3, which encode amino acids 33-105 of the INPP5K catalytic domain, and frameshift between exon 1 and remaining exons downstream of the deletion. Intercrosses between *Inpp5k*$^{\Delta/+}$ mice failed to yield any live *Inpp5k*$^{\Delta/\Delta}$ newborns, confirming previously published results indicating that total INPP5K

inactivation in mouse is embryonic lethal (Table S1) (Ijuin et al., 2008). *Inpp5k*$^{flox/+}$ Vav-Cre and *Inpp5k*$^{flox/flox}$ Vav-Cre (VAV-CRE) mice were obtained by crossing *Inpp5k*$^{flox/+}$ mice with mice expressing the Cre recombinase in all hematopoietic cells under the control of the murine Vav promoter. The INPP5K protein was absent from blood leukocytes isolated from VAV-CRE mice, confirming the efficiency of the recombination in these cells (Figure S1B). Blood leukocytes concentration was significantly decreased in VAV-CRE mice, as compared with control mice (Figure S2A). This alteration was mainly a consequence of a very severe decrease in total blood lymphocytes concentration. Decreased concentrations of basophils and increased concentrations of neutrophils and monocytes were also detected in VAV-CRE blood. Circulating red cells and platelets concentrations were normal in VAV-CRE mice. Flow cytometry analysis on blood lymphocytes indicated that concentrations of circulating $CD19^+$ B as well as of $CD3^+$, $CD4^+$ and $CD8^+$ T cells were significantly decreased in VAV-CRE mice compared with control mice (Figure S2B). Levels of circulating IgM, IgG and IgA were extremely low in the blood of VAV-CRE mice (Figure S2C). For this reason and because the INPP5K protein is expressed at all stages during B cell development in the bone marrow (Figure S3), we focused our study on the role of INPP5K in B cells and their precursors (Figure S4A). In the bone marrow of VAV-CRE mice, counts of multipotent and oligopotent progenitors, including multipotent progenitors, common myeloid progenitors and common lymphoid progenitors, were normal compared with control mice (Figure S5). Yet, loss of INPP5K resulted in a significant decrease in $B220^+$ B cells and in a complex pattern of alterations of B cell differentiation in the bone marrow (Figure S6 and Figure S4B-C). Indeed, cell counts were increased in fraction A and decreased in fraction B of VAV-CRE mice, as compared with control mice. This pattern is consistent

with a partial blockade at the transition between these 2 subsets (Figure S4C). Indeed, numbers of B cell progenitors in fractions C/C' were normal in VAV-CRE mice, but severely decreased in fractions D, E and F, compared with control mice (Figure S4C). In the spleen of VAV-CRE mice, total $CD19^+$ B cell counts and counts of T1, T2, FO and MZ B cell subsets as well as of plasmablasts were significantly decreased, compared with control mice (Figures S4D and S7). Counts of plasma cells were similar in VAV-CRE and control mice (Figure S7). In order to exclude that *Inpp5k* inactivation in hematopoietic cells other than B cells indirectly contributed to the B cell phenotype detected in VAV-CRE mice, we generated *Inpp5k*$^{flox/flox}$ MB1-Cre mice in which the Cre recombinase is expressed exclusively in B cells under the control of the murine CD79A promoter. In *Inpp5k*$^{flox/flox}$ MB1-Cre mice, the levels of INPP5K protein in fraction A were as high as in control mice, but reduced in fractions B and C/C', in agreement with published data showing that the expression of the Cre recombinase in MB1-Cre mice begins at the transition between fractions A and B (Figure S8A). Accordingly, cell count in fraction A was similar in *Inpp5k*$^{flox/flox}$ MB1-Cre and control mice (Figure S8B). Cell count in fraction B was significantly increased in *Inpp5k*$^{flox/flox}$ MB1-Cre mice compared to control mice, similarly to fraction A in VAV-CRE mice. In contrast with fraction B of VAV-Cre mice where cell counts were decreased compared to control mice, cell count in fractions C/C' was similar in *Inpp5k*$^{flox/flox}$ MB1-Cre and control mice (Figure S8B). We suspect this difference between fraction B of VAV-Cre and fractions C/C' of *Inpp5k*$^{flox/flox}$ MB1-Cre mice may be the result of a less efficient inactivation of the *Inpp5k* gene in fractions C/C' of MB1-Cre mice (Figures S6-S8A). This may also relate to the impossibility to simply define cell counts specifically in fraction C by flow cytometry, given that fractions C and C' have the same $B220^+CD43^+BP\text{-}1^+HSA^+$ cell surface

phenotype in Hardy's nomenclature despite different survival, proliferative and signaling features (Hardy, R. R., et al., 2007). Like in VAV-CRE mice, cell counts in fractions D, E and F were significantly decreased in *Inpp5k*$^{flox/flox}$ MB1-Cre mice compared to control mice, as well as blood IgM and IgG immunoglobulins levels (Figure S8B-C).

Altogether, our results indicate that *Inpp5k* inactivation in hematopoietic cells results in alterations in B cell differentiation and maturation at critical stages known to be controlled by the IL7R/PAX5 signaling pathway (fractions A/B) and by the cell surface expression of the pre-BCR (fractions C-C'/D) and of the BCR (fractions E and F, and splenic B cell subsets). They also indicate that *Inpp5k* inactivation specifically in the B cell lineage is sufficient to reproduce most of these alterations, supporting an intrinsic role of INPP5K during B cell development. In subsequent steps of this study, we focused on the alterations observed in fractions A and B during early bone marrow B cell differentiation in VAV-CRE mice and on the role of INPP5K in the IL7R/PAX5 signaling pathway.

**Supplementary Material 3:**

Since PAX5 is known to control $D_H$–$J_H$ and distal $V_H$–$D_HJ_H$ rearrangements at the IgH locus (Ebert, A., et al., 2011; Fuxa, M., et al., 2004; Hesslein, D. G. T., et al., 2003; Nutt, S. L., et al., 1997), we compared these recombination events in VAV-CRE and control bone marrow B cells. Reduced PAX5 expression in bone marrow VAV-CRE B cells was indeed associated with a decreased intensity of the PCR signal corresponding to the recombined $D_H$-$J_H$ and distal $V_H$J558-$D_HJ_H$ amplicons (Figure S11). As expected from previous reports, the proximal $V_H$7183-$D_HJ_H$ recombination, which is PAX5-independent, was not affected in VAV-CRE mice (Figure S11).

**Supplementary Material 4:**

**Loss of INPP5K results in altered membrane and cytoskeletal organization:**

Concomitantly to changes in IL7R dynamic structure, binding of IL7 to its receptor induces an increased number of $GM1^+$ membrane microdomains at the cell surface and the formation of an actin microfilament meshwork under the plasma membrane, which anchors the IL7-activated receptor and thus stabilizes the formation of the cytoplasmic signaling complex. Microtubules are then formed that cross the cytoplasm and reach the nuclear membrane within a few minutes after addition of IL7. Finally, p-STAT5 is carried along these newly formed microtubules toward the nucleus (Tamarit, B., et al., 2013). The impact of the loss of INPP5K on membrane and cytoskeletal organization was analyzed in basal and IL7-stimulated conditions. First, membrane microdomains were labeled through ganglioside GM1 with cholera toxin B (CtxB) tagged with AF488, in order to monitor their number, volume and GM1 staining intensity at the surface of VAV-CRE and control $B220^+CD43^+$ bone marrow B cells (Figure S15A). In control B cells, an increased number of $GM1^+$ microdomains was detected 10 min after addition of IL7, as compared with non-stimulated condition (Figure S15A). In addition, a decreased $GM1^+$ microdomain volume associated with an increased GM1 staining intensity was observed after addition of IL7, as compared with the basal condition, similarly to results obtained in IL7-stimulated human $CD4^+$ T cells (Tamarit , B., et al., 2013). These latter changes reached a peak 2 min after IL7 stimulation (Figure S15A). In VAV-CRE B cells, number of $GM1^+$ microdomains was normal in basal condition and slightly increased 2 and 10 min after addition of IL7, as compared with control B cells (Figure S15A). By contrast, their volume and GM1 staining intensity were already significantly altered before IL7

stimulation. Interestingly, addition of IL7 did not dramatically modify these 2 parameters, on the contrary to control B cells (Figure S15A). Second, reorganization of the actin and tubulin cytoskeletons was analyzed in $B220^{+}CD43^{+}$ bone marrow B cells before and after IL7 addition, as previously described for T cells (Tamarit, B., et al., 2013). An obvious difference was observed in actin organization 2 min after IL7 addition: a reorganization of the cortical actin skeleton was already clearly detected in VAV-CRE B cells while not yet visible in control B cells. This indicates that inactivation of INPP5K accelerates actin skeleton reorganization (Figure S15B). By contrast, no difference in actin staining was observed between VAV-CRE and control B cells before or 10 min after IL7 stimulation. As expected from the literature (Tamarit, B., et al., 2013), a significant number of microtubules formed in control B cells 2 and 10 min after addition of IL7 (Figure S15C). On the contrary, in VAV-CRE B cells, tubulin staining was diffuse throughout the cytoplasm, forming only very few microtubules of low intensity staining after addition of IL7 (Figure S15C).

Altogether, these results indicate that inactivation of INPP5K in bone marrow B cells results in altered $GM1^{+}$ microdomains and cytoskeletal organization. Interestingly, the volume and $GM1^{+}$ intensity of microdomains were already altered in basal conditions and remained largely unchanged after IL7 addition, like frozen at an intermediate level between basal and IL7-stimulated conditions in control B cells, and thus mimicking some of the structural alterations of the IL7R observed in VAV-CRE B cells.

**Supplementary Material 5:**

Before studying the effects of INPP5K knockdown in the human T-ALL DND-41 cell line, we first analyzed the impact of *Inpp5k* gene knock-out on blood and splenic T cells in

*Inpp5k*$^{flox/flox}$ Vav-Cre and *Inpp5k*$^{flox/flox}$ CD4-Cre mice, where *Inpp5k* is inactivated in all hematopoietic cells and specifically in the T cell lineage, respectively (Figure S16). In both mice, blood and splenic $CD3^+$, $CD3^+CD4^+$ and $CD3^+CD8^+$ T cell concentrations and numbers were significantly decreased compared to control mice, indicating that INPP5K also plays an intrinsic and important role in T lymphocytes in mice. Second, the expression of INPP5K was analyzed in human T and B lymphocytes. Transcriptomic and RNA seq analyses in public datasets showed that the INPP5K mRNA is present in all T and B lymphocyte subsets in human, and at all stages during differentiation of these cells (https://www.immgen.org/, https://genevestigator.com/, https://servers.binf.ku.dk/bloodspot/?gene=INPP5K&dataset=DMAP). A representative image of human INPP5K mRNA expression during T and B cell differentiation is presented in Figure S17A. Flow cytometry analyses revealed that both human blood $CD19^+CD20^+$ B cells and $CD3^+CD4^+$ T cells expressed high level of INPP5K protein (Figure S17B). Third, having demonstrated that INPP5K plays an important and intrinsic role in mouse T cells and that INPP5K is expressed in human T cells, the effects of INPP5K knockdown was investigated in the human T-ALL DND-41 cells line, which carries the constitutively activated p.Leu242_Leu243 insLeuSerArgCys IL7Rα chain insertion mutation, among other mutations in other signaling pathways. Five lentiviruses expressing different shRNAs directed against the human *INPP5K* mRNA were used to transduce DND-41 cells. With the most efficient shRNA anti-*INPP5K*, the residual INPP5K signal was ~25% of the signal observed in control shRNA/Mock-transduced DND-41 cells (Figure S18A). Despite this relatively high residual expression of INPP5K protein, basal levels of p-STAT5$^{Y694}$ and anti-apoptotic BCL-2 proteins were downregulated in DND-41 cells upon INPP5K silencing (Figure S18B-C).

**Table S1: Homozygous deletion of exons 2 and 3 of the mouse *Inpp5k* gene results in embryonic death.** Female *Inpp5k*$^{\Delta/+}$ mice were mated with male *Inpp5k*$^{\Delta/+}$ mice and followed every day before and after delivery. Newborns were counted every day and genotyped between 18 and 23 days after birth by PCR.

| **Couple (♂ x ♀):** | **Newborns genotype** | **Observed number (%)** | **Expected %** |
|---|---|---|---|
| *Inpp5k*$^{\Delta/+}$ x *Inpp5k*$^{\Delta/+}$ | ***Inpp5k*$^{+/+}$** | 12/42 (**28,6**) | 25 |
| | ***Inpp5k*$^{\Delta/+}$** | 30/42(**71,4**) | 50 |
| | ***Inpp5k*$^{\Delta/\Delta}$** | 0/42 (**0**)*** | 25 |

Statistics (Student's *t*-test): ***: P<0.001.

**Supplementary figure legends**

**Figure S1: Generation of *Inpp5K*$^{flox/+}$ mutant mouse. A.** The murine wild type, targeted and conditional knockout (KO) *Inpp5k* alleles are represented. Orange boxes denote exons; the blue and the yellow lines represent the homology arms of the targeting vector and the conditional knockout (CKO) region, respectively; purple triangles are LoxP sites and pink and white striped boxes are Frt sites. The targeting vector contains 2 cassettes: the first with a En2 splice acceptor (SA) site followed by an internal ribosome entry site (IRES) and a lacZ gene, the second with a human β actin promoter (hBactp) followed by the neomycin phosphotransferase gene (Neo). The CKO allele is represented after Flp recombination. **B.** INPP5K protein expression was analyzed by Western blotting on blood leukocytes protein extracts isolated from 2 controls (WT) and 2 VAV-CRE mice. Vinculin was used as a loading control protein.

**Figure S2: Loss of INPP5K protein in VAV-CRE mice induces severe blood leukocytes and immunoglobulins alterations. A.** Flow cytometry analysis and quantification of *Inpp5k*$^{flox/flox}$ (WT, blue columns) and *Inpp5k*$^{flox/flox}$ Vav-Cre (VAV-CRE, grey columns) blood cells concentration using a FC 500 Beckman Coulter (n=9 mice per group). **B.** Facs analysis and quantification of WT and VAV-CRE $CD19^+$, $CD3^+$, $CD3^+CD4^+$ and $CD3^+CD8^+$ blood lymphocyte concentrations (n=12 mice per group). Left panel: morphology graphics (SSC/FSC) and blood lymphocyte staining strategy; right panels: quantification of blood lymphocytes. **C.** ELISA analysis of WT (blue columns) and VAV-CRE (grey columns) blood IgM, IgG and IgA immunoglobulins concentrations. Results represent individual mice and means ± SEM. *P* values were calculated using unpaired nonparametric *t* test. N.S.: *P*>0,05; *: *P*<0,05; **: *P*<0,01; ***: *P*<0,001; ****: *P*<0,0001.

**Figure S3: INPP5K protein expression in bone marrow B cells from control mice.** Expression of the INPP5K protein was analyzed by flow cytometry in fractions (Fr.) A to F of bone marrow B cells isolated from control mice. Results represent individual mice (n=10 to 12 mice per group) and means ± SEM of mean fluorescence intensity (MFI).

**Figure S4: *Inpp5k* inactivation results in altered B cell differentiation and maturation.** A. Representative figure of early B cell development in the mouse bone marrow according to Hardy's nomenclature. The different stages, from fraction (Fr.) A (PrePro B) to F (mature B cells) as well as essential receptors driving the differentiation (IL7R, Pre-BCR and BCR) are represented. B. Numbers of bone marrow $B220^+$ B cells were analyzed by flow cytometry in control (WT, blue columns) and VAV-CRE (grey columns) mice. Left panels: morphology graphic (SSC/FSC) and staining strategy for $B220^+$ bone marrow B cells; right graph: total numbers of bone marrow $B220^+$ B cells isolated from 2 femurs and 2 tibias. Results represent individual mice (n=7 mice per group) and means ± SEM. C. Flow cytometry analysis of control (WT, blue columns) and VAV-CRE (grey columns) bone marrow B cells development according to Hardy's nomenclature. Upper panels: staining strategy for the different stages of early B cell development in the bone marrow: fraction (Fr.) A ($B220^+CD43^+BP\text{-}1^-HSA^-$); fraction B ($B220^+CD43^+BP\text{-}1^-HSA^+$); fractions C/C' ($B220^+CD43^+BP\text{-}1^+HSA^+$); fraction D ($B220^+CD43^-IgM^-IgD^-$); fraction E ($B220^+CD43^-IgM^+IgD^-$) and fraction F ($B220^+CD43^-IgM^+IgD^+$). Lower graphs: numbers of B cells in each fraction, according to their percentage and the total number of cells isolated from 2 femurs and 2 tibias. Results represent individual mice (n=15 mice per group) and means ± SEM. D. Flow cytometry analysis of control (WT, blue column) and VAV-CRE (grey column) splenic $CD19^+$ B cells numbers. Left panels: morphology graphic (SSC/FSC) and staining strategy for $CD19^+$

bone marrow B cells; right graph: total numbers of splenic $CD19^+$ B cells. Results represent individual mice (n=17 mice per group) and means ± SEM. *P* values were calculated using unpaired nonparametric test. N.S.: *P*>0,05; *: *P*<0,05; **: *P*<0,01; ***: *P*<0,001; ****: *P*<0,0001.

**Figure S5: Normal numbers of hematopoietic progenitor cells in the absence of INPP5K.** Numbers of multipotent, common myeloid and common lymphoid progenitors were analyzed by flow cytometry in control (WT, blue columns) and VAV-CRE (grey columns) bone marrows. Results represent individual mice (n=3 to 6 mice per group) and means ± SEM. N.S.: *P*>0,05.

**Figure S6**: **Markedly reduced expression of INPP5K protein in VAV-CRE B cell precursors.** Representative MFI histograms of INPP5K protein expression in bone marrow B cells precursors (fractions (Fr.) A, B and C/C') from control (WT, blue areas) and VAV-CRE (grey areas) mice. The black areas are representative of the fluorochrome-labelled secondary antibody alone, as negative control ($C^-$). INPP5K protein expression was analyzed after plasma membrane permeabilization.

**Figure S7: Altered B cell maturation in the spleen of VAV-CRE mice.** Flow cytometry analysis of control and VAV-CRE splenic B cell maturation. Left panels: staining strategy to identify the different splenic B cell subsets: Transitional 1 (T1, $CD19^+CD23^-CD21^-IgM^+$); Transitional 2 (T2, $CD19^+CD23^+CD21^+IgM^+$); Follicular (FO B, $CD19^+CD23^+CD21^{Int}IgM^{int}$); Marginal Zone (MZ B, $CD19^+CD23^-CD21^+IgM^+$); Plasmablasts (PB, $B220^+CD19^+CD138^+$) and Plasma cells (PC, $B220^+CD19^-CD138^+$). Right graphs: B cell numbers in each splenic subset of control (WT, blue columns) and VAV-CRE (grey columns) mice. Results represent individual mice (n=5 to 8 mice per

group) and means ± SEM. *P* values were calculated using unpaired nonparametric *t* test. N.S.: *P*>0,05; **: *P*<0,01; ***: *P*<0,001; ****: *P*<0,0001.

**Figure S8: Reduced expression of INPP5K protein in *Inpp5k*$^{flox/flox}$ MB1-CRE mice results in altered B cell differentiation and decreased blood levels of IgM and IgG immunoglobulins. A.** Representative MFI histograms of INPP5K protein expression in bone marrow B cells precursors (fractions (Fr.) A, B and C/C') from control (WT, blue areas) and *Inpp5k*$^{flox/flox}$ MB1-CRE (MB1-CRE, green areas) mice. The black areas are representative of the fluorochrome-labelled secondary antibody alone, as negative control ($C^-$). INPP5K protein expression was analyzed after plasma membrane permeabilization. **B.** Flow cytometry analysis of control (WT, blue columns) and *Inpp5k*$^{flox/flox}$ MB1-CRE (MB1-CRE, green columns) bone marrow B cell development according to Hardy's nomenclature. Left panels: staining strategy for the different stages of early B cell development in the bone marrow: fraction A ($B220^+CD43^+BP\text{-}1^-HSA^-$); fraction B ($B220^+CD43^+BP\text{-}1^-HSA^+$); fractions C/C' ($B220^+CD43^+BP\text{-}1^+HSA^+$); fraction D ($B220^+CD43^-IgM^-IgD^-$); fraction E ($B220^+CD43^-IgM^+IgD^-$) and fraction F ($B220^+CD43^-IgM^+IgD^+$). Right graphs: numbers of B cells in each fraction, according to their percentage and the total number of cells isolated from 2 femurs and 2 tibias. Results represent individual mice (n=5 to 12 mice per group) and means ± SEM. *P* values were calculated using unpaired nonparametric *t* test. N.S.: *P*>0,05; *: *P*<0,05; ***: *P*<0,001. **C.** ELISA analysis of blood control (WT, blue columns) and *Inpp5k*$^{flox/flox}$ MB1-CRE (MB1-CRE, green columns) IgM and IgG immunoglobulins concentrations. Results represent individual mice (n=11 mice per group) and means ± SEM. *P* values were calculated using unpaired nonparametric *t* test. ****: *P*<0,0001.

**Figure S9: Normal levels of IL7Rα, p-IL7Rα$^{Y449}$, γc, AKT, STAT5 JAK1 and JAK3 proteins in bone marrow VAV-CRE B cells. A.** Expression of IL7Rα, γc, STAT5, JAK1 and JAK3 proteins was analyzed by flow cytometry in cells of fractions A and B from control (WT, blue columns) and VAV-CRE (grey columns) mice. Results represent MFI normalized to WT mean MFI (IL7Rα) and MFI (γc, JAK1, JAK3 and STAT5) in individual mice (n=3 to 6 mice per group), as well as means ± SEM. Expression of AKT protein was analyzed by Western blotting in bone marrow B220$^+$ B cells from WT and VAV-CRE mice. HSP90 was used as a loading control in the blot experiment. **B.** Phosphorylation of the IL7Rα chain at Y$^{449}$ was analyzed by flow cytometry with a p-IL7Rα$^{Y449}$ antibody in plasma membrane-permeabilized bone marrow B cells from control (WT, blue areas and lines) and VAV-CRE (grey areas and lines) mice. Left panels: representative MFI histrograms of p-IL7Rα$^{Y449}$ in fraction A (above) and B (below) B cells before (0) and 2 or 10 min after *ex-vivo* addition of IL-7 (2ng/ml) at 37°C. Right graphs: quantitative analysis of p-IL7Rα$^{Y449}$ signal in fractions A (above) and B (below) B cells from control (WT, blue lines) and VAV-Cre (grey lines) mice, normalized to WT mean MFI before IL-7 stimulation (T0). Results represent means ± SEM (n=8-9 mice per group). *P* values were calculated using unpaired nonparametric *t* test. N.S.: *P*>0,05, *: *P*<0,05.

**Figure S10: Altered recombination at the IgH locus in VAV-CRE mice:** PAX5-dependent $D_H$-$J_H$ and $V_H$J558-$D_HJ_H$ as well as PAX5-independent $V_H$7183-$D_HJ_H$ rearrangements were analyzed by PCR with specific primers using genomic DNA purified from WT and VAV-CRE B220$^+$CD43$^+$ bone marrow B cells as templates. PCR amplification of the *Gapdh* gene served as a positive control (C$^+$). Genomic DNA isolated from facs-sorted CD11b$^+$Ly6G$^+$ bone marrow neutrophils (C$^-$) served as a negative control. Results represent the prominent amplicons obtained from 2 WT and 2 VAV-CRE mice

and correspond to the amplified $D_H$-$J_H$3, $V_H$J558-$D_HJ_H$ and $V_H$J7183-$D_HJ_H$ segments at the IgH locus. MW: molecular weight markers.

**Figure S11: Reduced expression of INPP5K protein in *Inpp5k*$^{flox/flox}$ MB1-CRE mice results in decreased PAX5 and EBF1 levels in B cells precursors.** PAX5 and EBF1 protein expression was analyzed by flow cytometry after plasma and nuclear membranes permeabilization of control (WT, blue columns) and *Inpp5k*$^{flox/flox}$ MB1-CRE (MB1-CRE, green columns) cells from fraction B. Graphs represent the quantitative expression of PAX5 (left) and EBF1 (right) proteins after MFI normalization to WT mean MFI. Results represent individual mice (n=6 mice per group) and means ± SEM. *P* values were calculated using unpaired nonparametric *t* test. **: *P*<0,01; ***: *P*<0,001.

**Figure S12: Positive and negative control conditions for indirect FRET experiments.** In order to define the maximal and the minimal FRET efficiency, $B220^+CD43^+$ bone marrow cells were sorted from control mice, incubated either with a primary rat anti-mouse JAK1 antibody and then with 2 secondary goat anti-rat IgG antibodies labeled with AF546 or AF488 (as positive control, $C^+$), or with primary rat anti-mouse JAK1 and rabbit anti-PAX5 antibodies and then with AF546-labeled goat anti-rat IgG and AF488-labeled goat anti-rabbit IgG secondary antibodies (as negative control, $C^-$). Left Panels: representative confocal pictures (63X) of energy transfer (FRET efficiency, upper 2 panels) between AF488- and AF546-labeled secondary antibodies; the corresponding nuclear staining (DAPI) is presented in the lower 2 panels. The rainbow scale represents the energy transfer between the two fluorophores, from 0 (blue) to 6 (white). Right graph: the quantitative energy transfer between AF488- and AF546-labeled secondary antibodies (FRET efficiency) is presented. Results represent individual cells and means ± SEM.

**Figure S13: Sequence alignment of the IL7Rα juxtamembrane cytoplasmic regions from different species.** Presence of a conserved positively-charged polybasic amino acid sequence in the juxtamembrane region of the IL7Rα cytoplasmic domain in different species. Box 1 and 2 (grey) represent the two JAK1 binding domains on the IL7Rα chain. The transmembrane region (green), hydrophobic (blue), positively (purple) and negatively (red) charged amino acids are represented.

**Figure S14: Mutational analysis of the 3 clusters of basic amino acids in the peptide present in the cytoplasmic juxtamembrane domain of the IL7Rα chain. A**. the 45 amino acid sequence of the wild type (WT) and the 3 mutated (Mut1, Mut2 and Mut3) peptides used in the assay. The hydrophobic (blue), positively (purple) and negatively (red) charged amino acids are represented. The nonpolar Alanine (A) introduced in one of the three clusters is represented in black. **B**. A tryptophan fluorescence emission spectrum assay was used to detect the binding of the WT, Mut1, Mut2 and Mut3 peptides to 10% acidic PtdIns(4,5)P2/90% zwitterionic POPC bicelles at different lipid concentrations. **C**. The graph represents the maximum wavelength difference plot relative to the zero point for each peptide-bicelle titration. All mutated peptides present an altered maximum wavelength shift compared to the WT peptide, meaning that all 3 polybasic amino acid clusters are important for binding to PtdIns(4,5)P2/POPC bicelles.

**Figure S15: Inpp5k inactivation results in altered membrane and cytoskeletal organization. A**. Left upper panels: representative confocal pictures (100X) of $GM1^{+}$ membrane microdomains stained with AF488-labeled Cholera Toxin B (CtxB, green) on $B220^{+}CD43^{+}$ B cells sorted from control and VAV-CRE mice before (0) and 2 or 10 min after *ex-vivo* addition of IL7 (2ng/ml) at 37°C. White scale bar: 1µm. Graphs: number,

volume and fluorescence intensity of $GM1^+$ microdomains ($GM1^+$ MD) were analyzed by confocal microscopy after staining with AF488-labeled CtxB in $B220^+CD43^+$ B cells sorted from control (WT, blue lines) and VAV-CRE (grey lines) mice before (0) and 2 or 10 min after *ex-vivo* addition of IL7 (2ng/ml) at 37°C. Results represent means ± SEM (n=30 cells from 3 mice per group). **B**-**C**. Representative confocal pictures (100X) of actin (red, B) and tubulin (green, C) staining of plasma membrane-permeabilized $B220^+CD43^+$ bone marrow B cells sorted from control (WT) and VAV-CRE mice before (0) and 2 or 10 min after *ex-vivo* addition of IL7 (2ng/ml) at 37°C. White arrows represent actin/tubulin polyperization. White scale bars: 1µm. *P* values were calculated using unpaired nonparametric t test. N.S.: *P*>0,05; *: *P*<0,05; **: *P*<0,01; ***: *P*<0,001; ****: *P*<0,0001.

**Figure S16: Loss of INPP5K protein in VAV-CRE and *Inpp5k*$^{flox/flox}$ CD4-Cre mice induces T cell alterations.** Flow cytometry analysis and quantification of blood (**A**, **C**) and splenic (**B**, **D**) $CD3^+$, $CD3^+CD4^+$ and $CD3^+CD8^+$ T cells in *Inpp5k*$^{flox/flox}$ (WT, blue columns), *Inpp5k*$^{flox/flox}$ Vav-Cre (VAV-CRE, grey columns) and *Inpp5k*$^{flox/flox}$ CD4-Cre (CD4-CRE, brown columns) mice (n=5 to 14 mice per group). Left panels: lymphocyte staining strategy; right panels: quantification of T lymphocytes. Results represent individual mice and means ± SEM. P values were calculated using unpaired nonparametric t test. *: P<0,05; **: P<0,01; ***: P<0,001.

**Figure S17: INPP5K expression in human lymphocytes: A.** INPP5K gene expression pattern at different lymphocyte maturation stages based on curated microarray data (from https://servers.binf.ku.dk/bloodspot/?gene=INPP5K&dataset=DMAP). Hematopoietic stem cell (HSC $CD133^+$ $CD34^{dim}$), mature B-cell class able to switch ($CD19^+$ $IgD^+$ $CD27^+$), $CD8^+$ Central Memory ($CD8^+$ $CD62L^+$ $CD45RA^-$), $CD8^+$ Effector

Memory ($CD8^+$ $CD62L^-$ $CD45RA^-$), $CD4^+$ Central Memory ($CD4^+$ $CD62L^+$ $CD45RA^-$), $CD4^+$ Effector Memory ($CD4^+$ $CD62L^-$ $CD45RA^-$), CMP (Common myeloid progenitor), GMP (Granulocyte/monocyte progenitor). **B**. Flow cytometry analysis of INPP5K protein in human blood $CD19^+CD20^+$ B cells and $CD3^+CD4^+$ T cells. The black areas are representative of the fluorochrome-labeled secondary antibody alone, as negative control ($C^-$). INPP5K protein expression was analyzed after plasma membrane permeabilization.

**Figure S18: INPP5K silencing in human T-ALL DND-41 cells carrying a constitutively activated IL7Rα chain insertion mutation downregulates basal levels of p-STAT5$^{Y694}$ and anti-apoptotic BCL-2 proteins.** INPP5K (**A**), p-STAT5$^{Y694}$ (**B**) and BCL-2 (**C**) signals were analyzed by flow cytometry in plasma membrane-permeabilized DND-41 cells transduced with shINPP5K or control mock shRNA (Mock). Representative MFI histograms are shown. $C^-$ is the background signal generated by the labeled secondary antibody alone.

**Figure S1**

**A**

Wildtype allele


Targeted allele

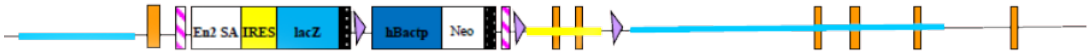


Conditional KO allele
(after Flp recombinaison)

LoxP site  Frt site  Exon  CKO region  Homology arm

**B**

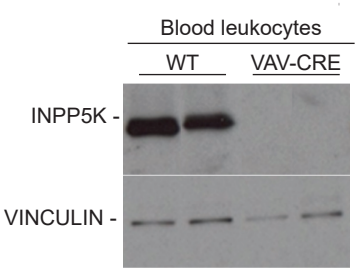

**Figure S2**

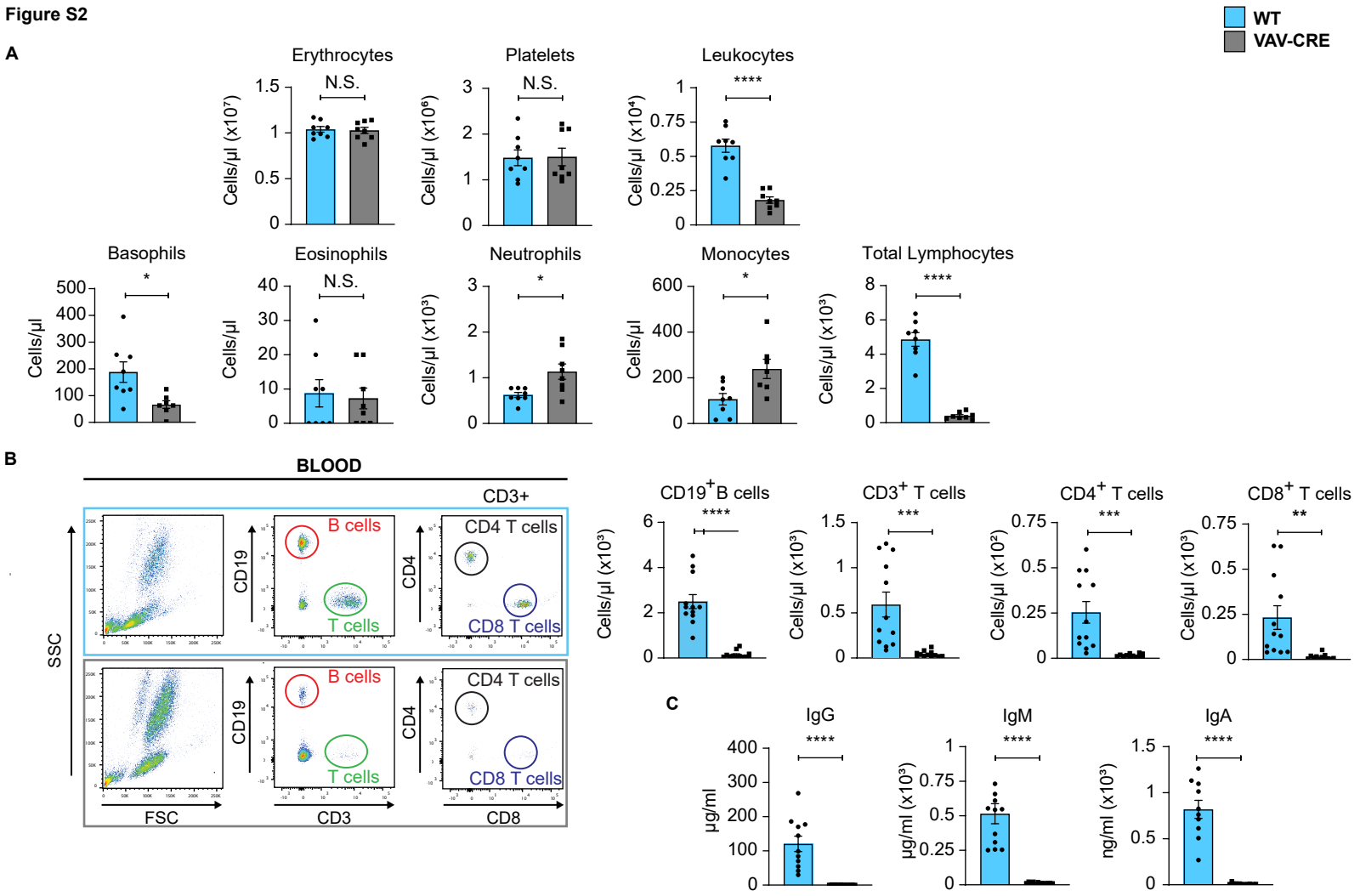
WT
VAV-CRE
A
Erythrocytes
N.S.
Cells/µl (x10⁷)
Platelets
N.S.
Cells/µl (x10⁶)
Leukocytes
****
Cells/µl (x10⁴)
Basophils
*
Cells/µl
Eosinophils
N.S.
Cells/µl
Neutrophils
*
Cells/µl (x10³)
Monocytes
*
Cells/µl
Total Lymphocytes
****
Cells/µl (x10³)
B
BLOOD
CD3+
SSC
FSC
CD19
B cells
T cells
CD4
CD4 T cells
CD8 T cells
CD3
CD8
CD19⁺B cells
****
Cells/µl (x10³)
CD3⁺ T cells
***
Cells/µl (x10³)
CD4⁺ T cells
***
Cells/µl (x10²)
CD8⁺ T cells
**
Cells/µl (x10³)
C
IgG
****
µg/ml
IgM
****
µg/ml (x10³)
IgA
****
ng/ml (x10³)

**Figure S3**

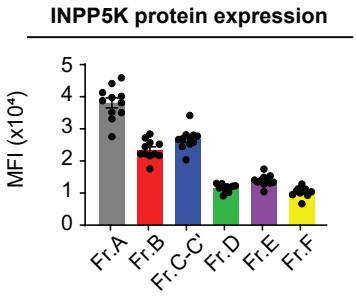
INPP5K protein expression
MFI (x10⁴)
5
4
3
2
1
0
Fr.A
Fr.B
Fr.C-C'
Fr.D
Fr.E
Fr.F

**Figure S4**

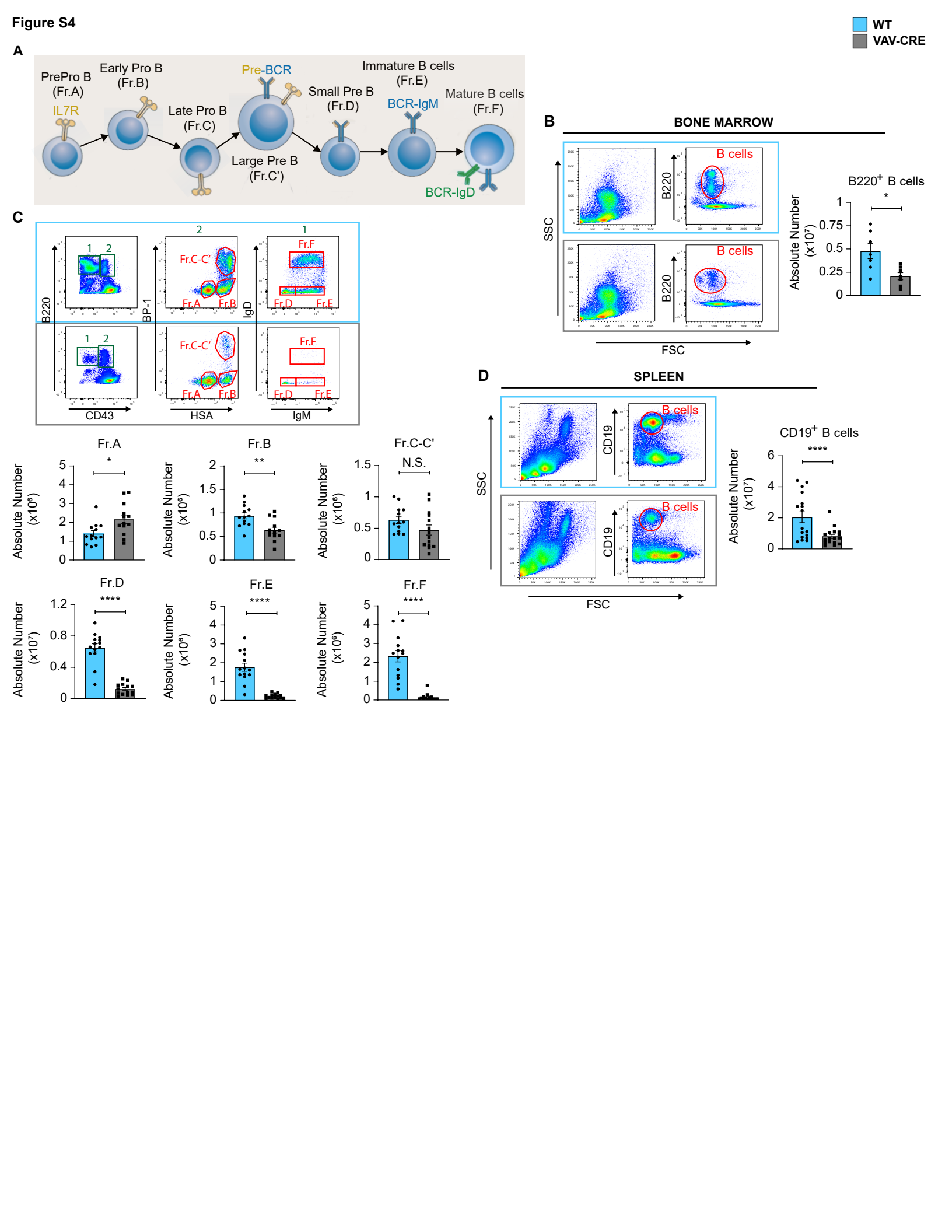
WT
VAV-CRE
A
PrePro B (Fr.A)
IL7R
Early Pro B (Fr.B)
Late Pro B (Fr.C)
Pre-BCR
Large Pre B (Fr.C')
Small Pre B (Fr.D)
Immature B cells (Fr.E)
BCR-IgM
Mature B cells (Fr.F)
BCR-IgD
B
BONE MARROW
B cells
B220
SSC
FSC
B220+ B cells
Absolute Number (x10⁷)
C
B220
BP-1
IgD
CD43
HSA
IgM
Fr.A
Fr.B
Fr.C-C'
Fr.D
Fr.E
Fr.F
Absolute Number (x10⁶)
Absolute Number (x10⁷)
N.S.
D
SPLEEN
CD19
CD19+ B cells

**Figure S5**

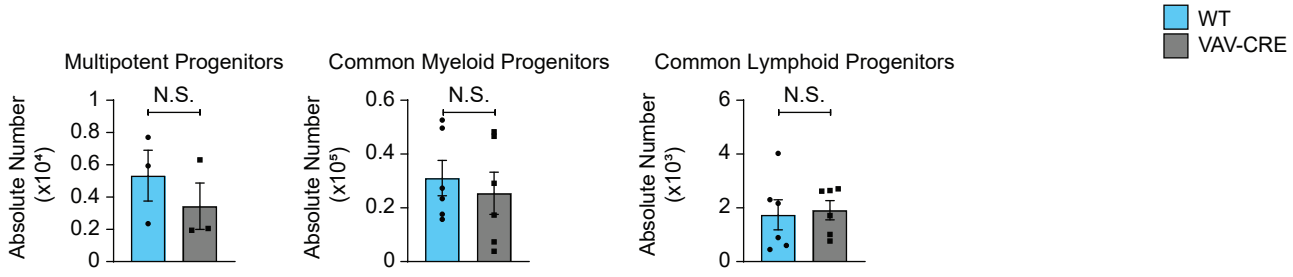
WT
VAV-CRE
Multipotent Progenitors
Common Myeloid Progenitors
Common Lymphoid Progenitors
N.S.
N.S.
N.S.
Absolute Number (x10⁴)
Absolute Number (x10⁵)
Absolute Number (x10³)
0
0.2
0.4
0.6
0.8
1
0
0.2
0.4
0.6
0
2
4
6

**Figure S6**

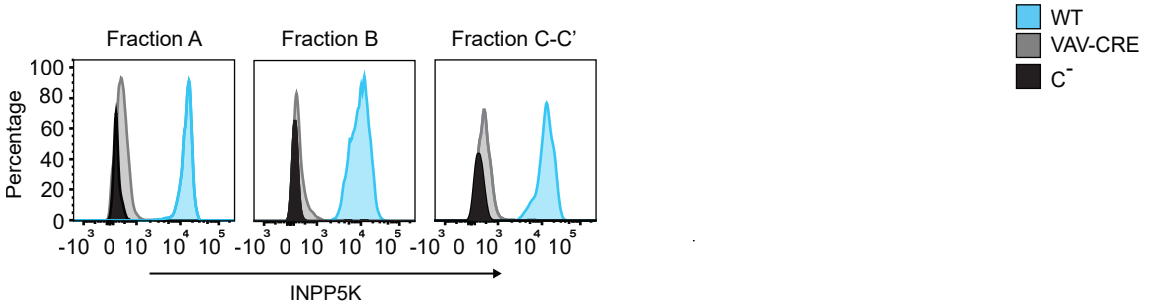
Fraction A
Fraction B
Fraction C-C'
WT
VAV-CRE
C-
Percentage
100
80
60
40
20
0
-10^3 0 10^3 10^4 10^5
INPP5K

**Figure S7**

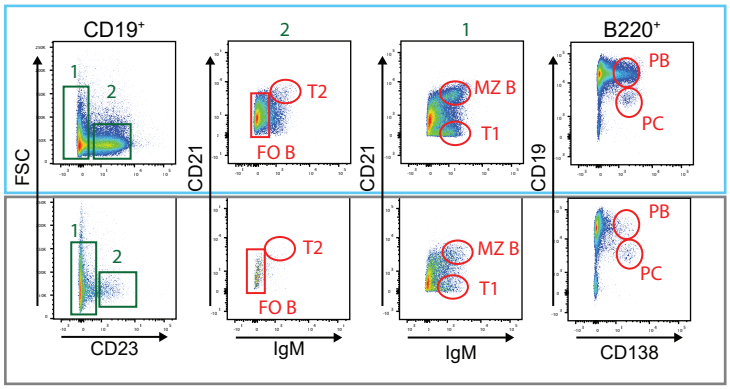
CD19⁺
2
1
B220⁺
FSC
CD21
CD21
CD19
1
2
T2
FO B
MZ B
T1
PB
PC
CD23
IgM
IgM
CD138

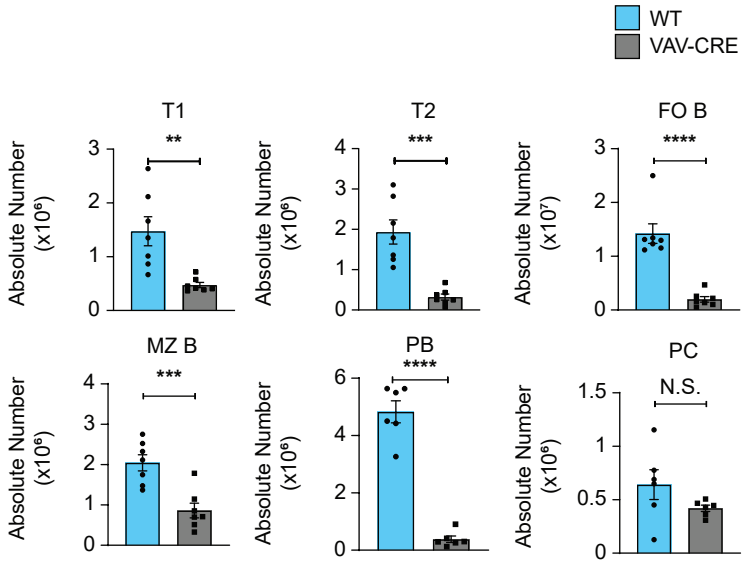
WT
VAV-CRE
T1
T2
FO B
MZ B
PB
PC
Absolute Number (x10⁶)
Absolute Number (x10⁷)
**
***
****
N.S.

**Figure S8**

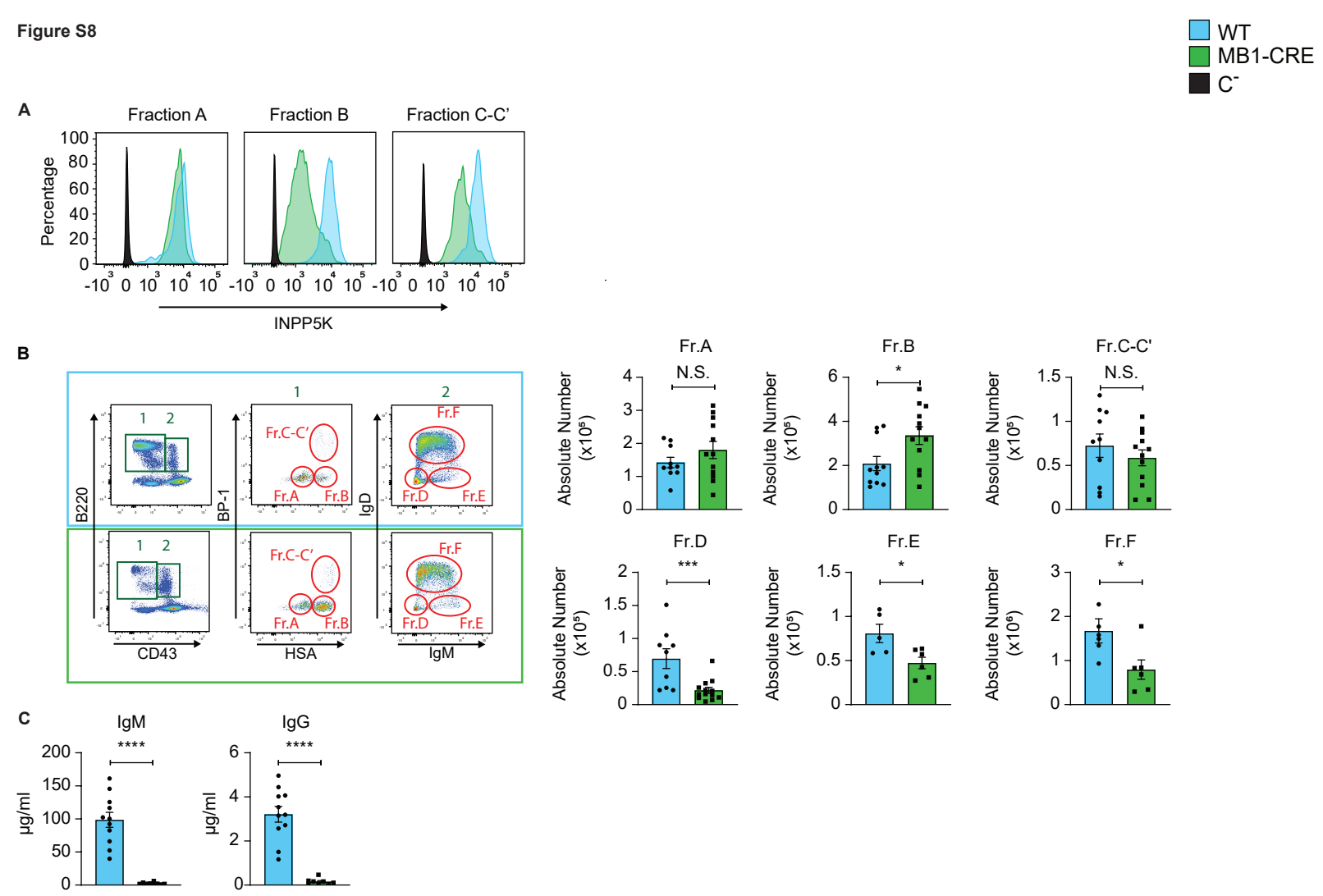
WT
MB1-CRE
C-
A
Fraction A
Fraction B
Fraction C-C'
Percentage
INPP5K
B
B220
BP-1
IgD
CD43
HSA
IgM
Fr.A
Fr.B
Fr.C-C'
Fr.D
Fr.E
Fr.F
Absolute Number (x10⁵)
Absolute Number (x10⁶)
N.S.
*
***
C
IgM
IgG
****
µg/ml

**Figure S9**

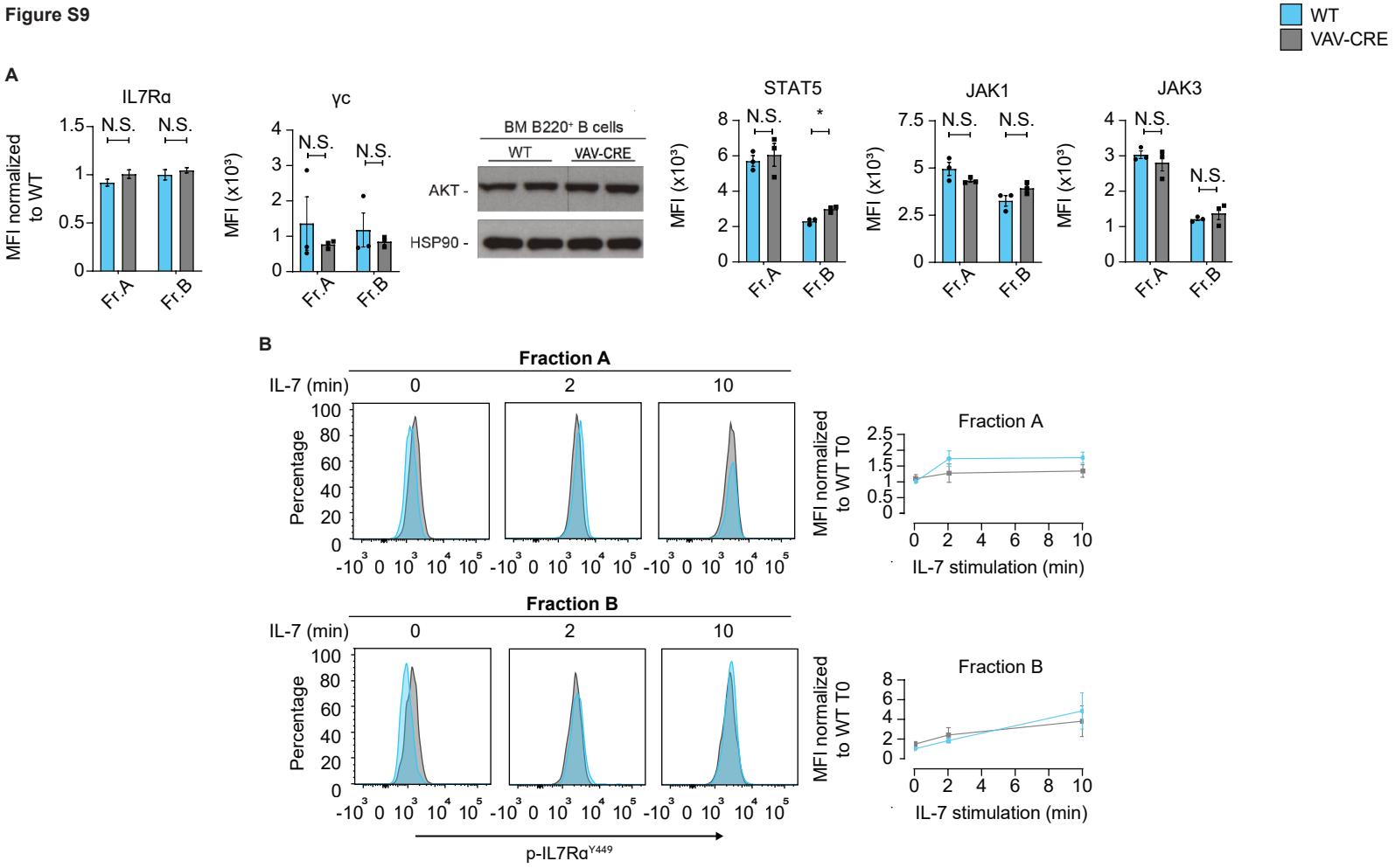
WT
VAV-CRE
A
IL7Rα
γc
BM B220⁺ B cells
WT
VAV-CRE
AKT -
HSP90 -
STAT5
JAK1
JAK3
MFI normalized to WT
MFI (x10³)
N.S.
*
Fr.A
Fr.B
B
Fraction A
Fraction B
IL-7 (min)
0
2
10
Percentage
MFI normalized to WT T0
IL-7 stimulation (min)
p-IL7Rα^Y449

**Figure S10**

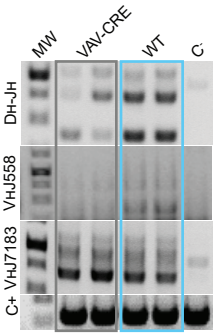


WT
VAV-CRE

**Figure S11**

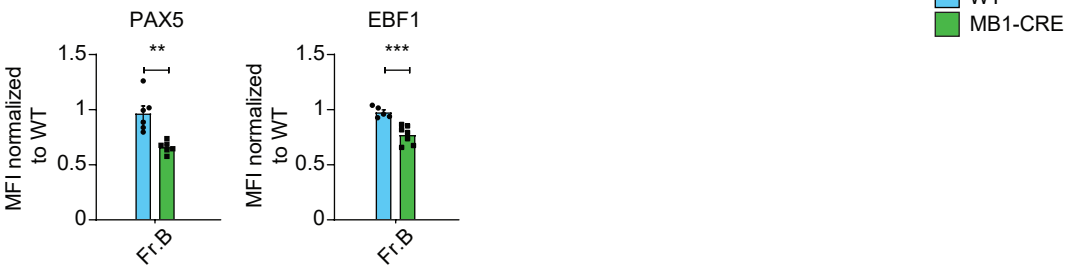

Figure S12

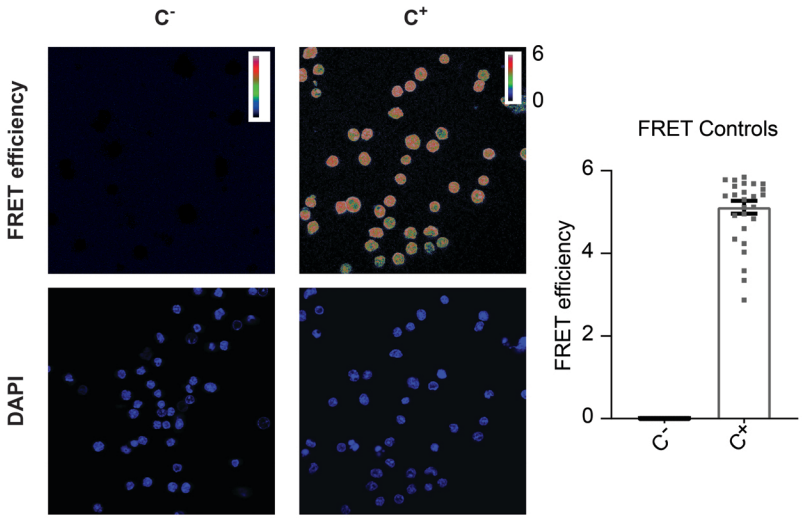
C-
C+
FRET efficiency
DAPI
6
0
FRET Controls
FRET efficiency
6
4
2
0
C-
C+

**Figure S13**

**The IL7Rα/CD127 chain :**

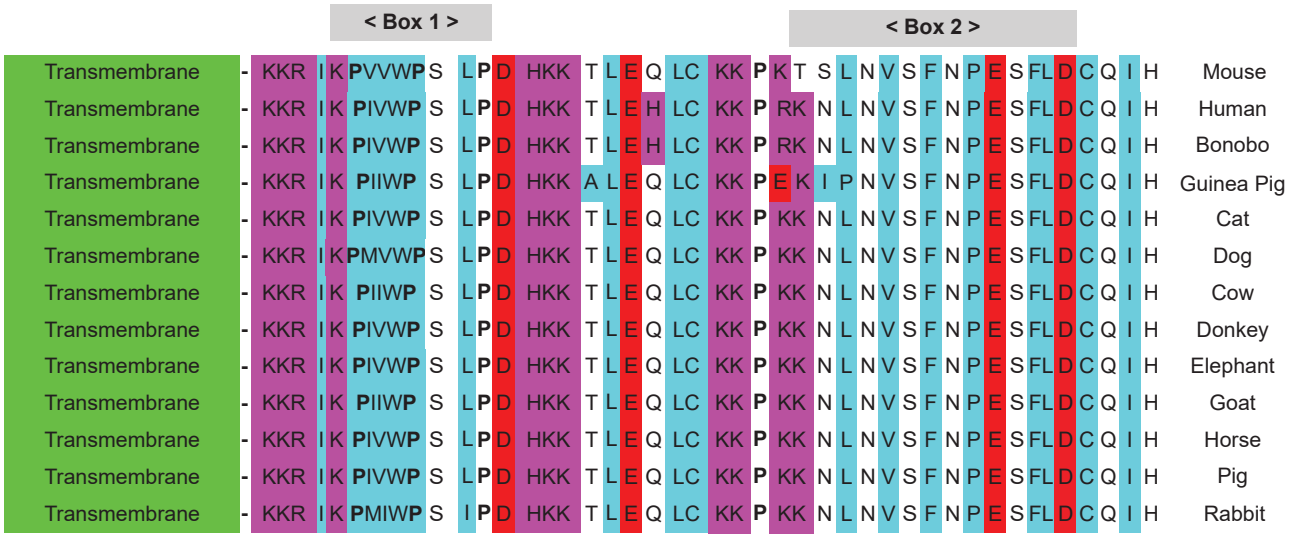


XX Transmembrane region

XX Hydrophobic amino acid

XX Positively charged amino acid

XX Negatively charged amino acid

**Figure S14**

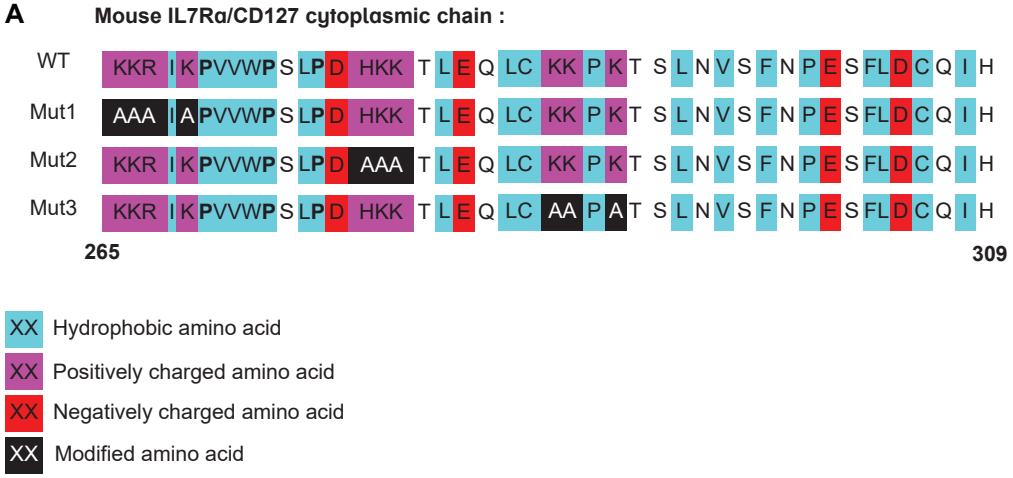
A
Mouse IL7Rα/CD127 cytoplasmic chain :
WT KKR I K PVVWP S LP D HKK T L E Q LC KK P K T S L N V S F N P E S FL D C Q I H
Mut1 AAA I A PVVWP S LP D HKK T L E Q LC KK P K T S L N V S F N P E S FL D C Q I H
Mut2 KKR I K PVVWP S LP D AAA T L E Q LC KK P K T S L N V S F N P E S FL D C Q I H
Mut3 KKR I K PVVWP S LP D HKK T L E Q LC AA P A T S L N V S F N P E S FL D C Q I H
265
309
XX Hydrophobic amino acid
XX Positively charged amino acid
XX Negatively charged amino acid
XX Modified amino acid

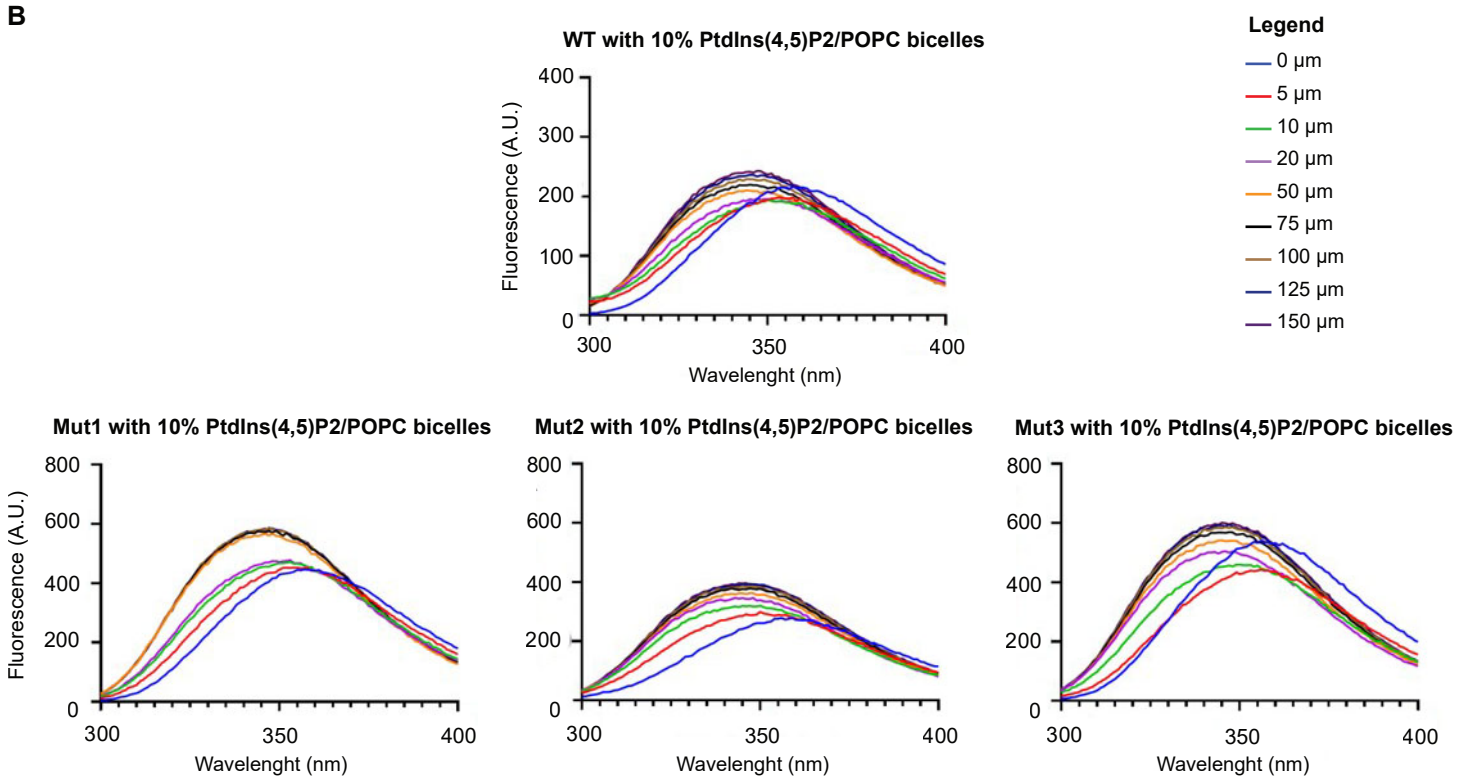
B
WT with 10% PtdIns(4,5)P2/POPC bicelles
Fluorescence (A.U.)
Wavelenght (nm)
Legend
0 µm
5 µm
10 µm
20 µm
50 µm
75 µm
100 µm
125 µm
150 µm
Mut1 with 10% PtdIns(4,5)P2/POPC bicelles
Mut2 with 10% PtdIns(4,5)P2/POPC bicelles
Mut3 with 10% PtdIns(4,5)P2/POPC bicelles

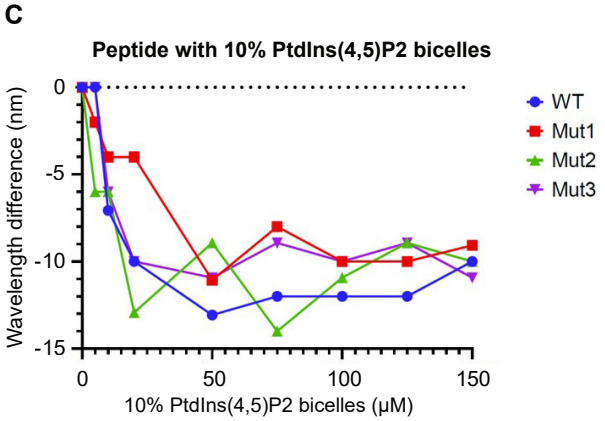
C
Peptide with 10% PtdIns(4,5)P2 bicelles
Wavelength difference (nm)
10% PtdIns(4,5)P2 bicelles (µM)
WT
Mut1
Mut2
Mut3

Figure S15

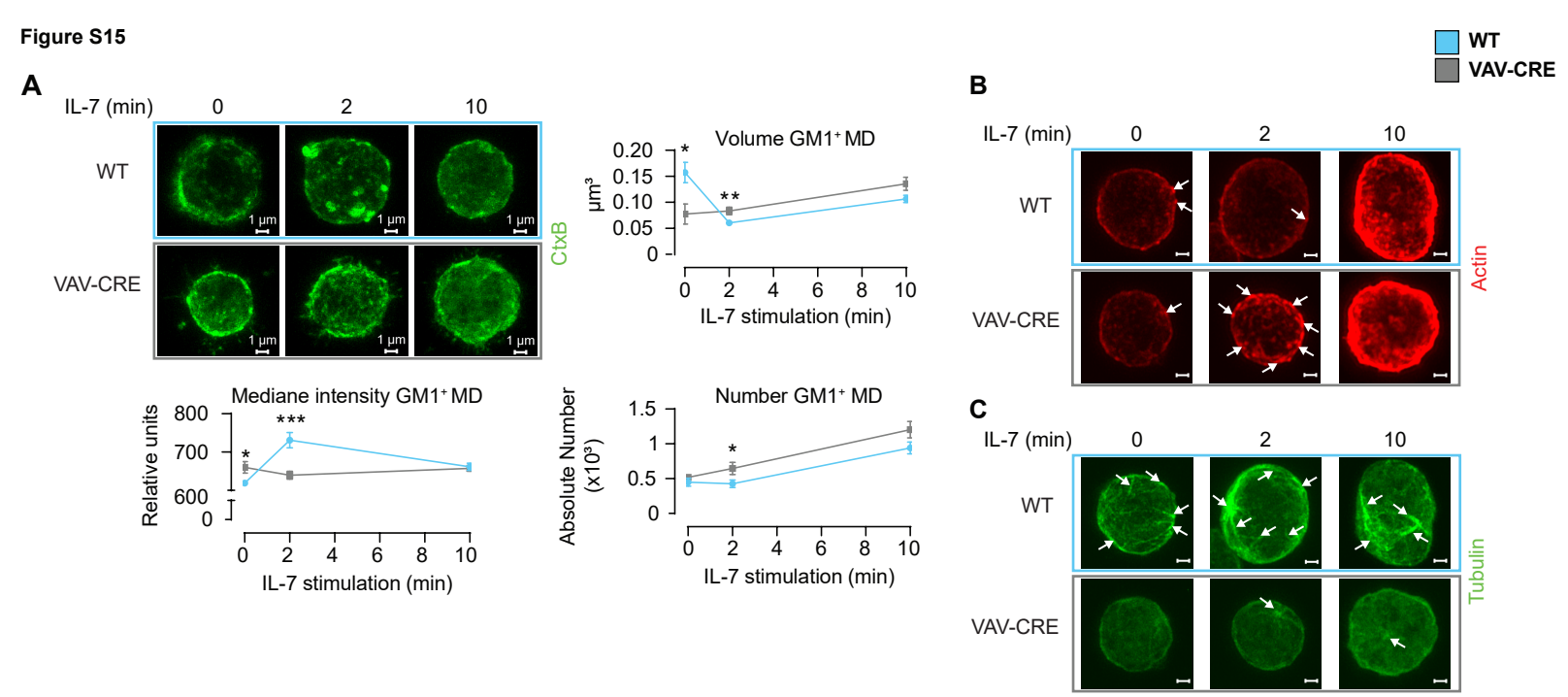
A
IL-7 (min)
0
2
10
WT
VAV-CRE
1 µm
CtxB
Volume GM1⁺ MD
µm³
0.20
0.15
0.10
0.05
0
*
**
0
2
4
6
8
10
IL-7 stimulation (min)
Mediane intensity GM1⁺ MD
Relative units
800
700
600
0
***
*
IL-7 stimulation (min)
Number GM1⁺ MD
Absolute Number (x10³)
1.5
1
0.5
0
*
IL-7 stimulation (min)
WT
VAV-CRE
B
IL-7 (min)
0
2
10
WT
VAV-CRE
Actin
C
IL-7 (min)
0
2
10
WT
VAV-CRE
Tubulin

Figure S16

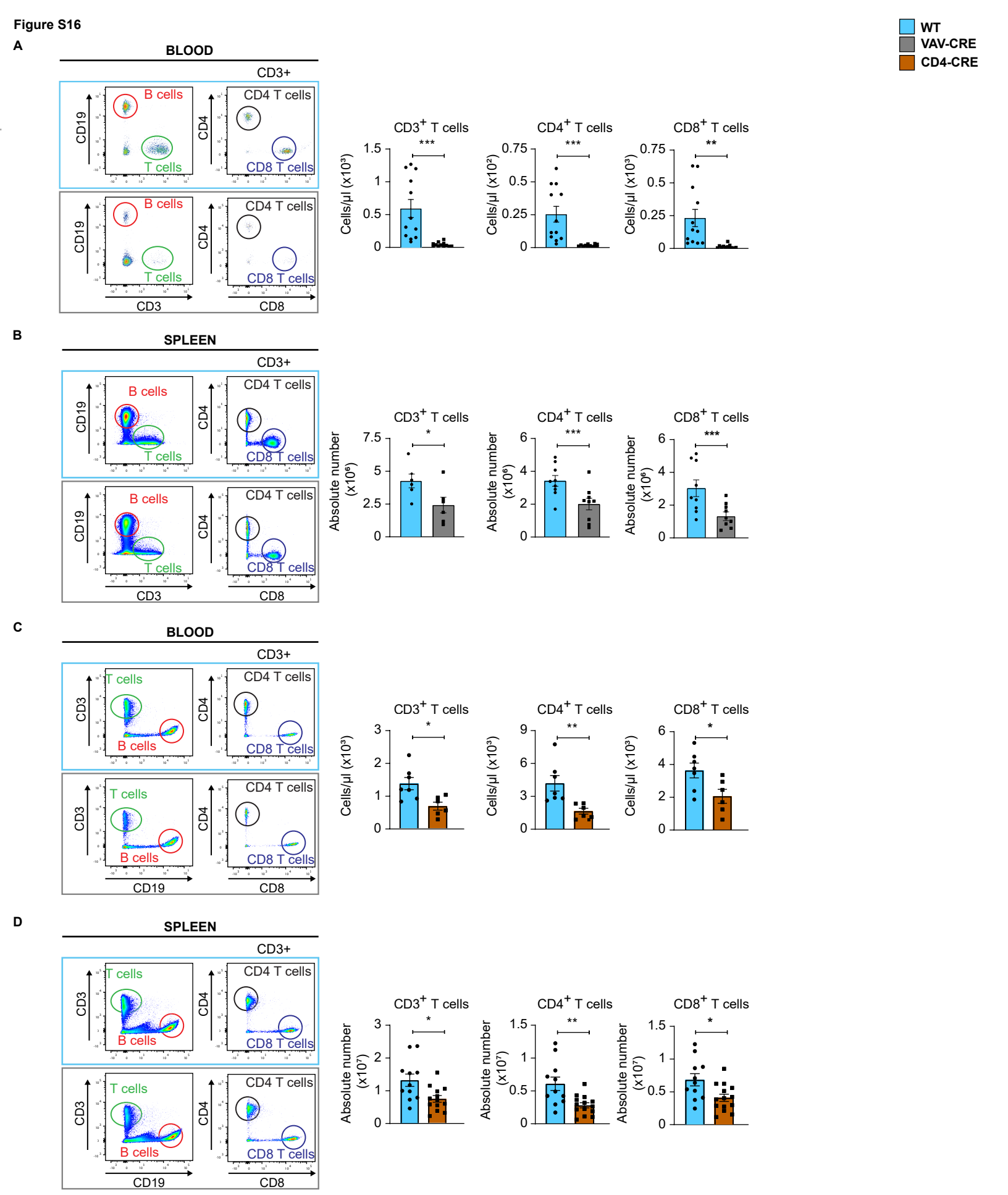
WT
VAV-CRE
CD4-CRE
A
BLOOD
CD3+
B cells
T cells
CD4 T cells
CD8 T cells
CD19
CD4
CD3
CD8
CD3+ T cells
CD4+ T cells
CD8+ T cells
Cells/µl (x10³)
Cells/µl (x10²)
***
**
B
SPLEEN
Absolute number (x10⁶)
*
C
BLOOD
Cells/µl (x10³)
D
SPLEEN
Absolute number (x10⁷)

Figure S17

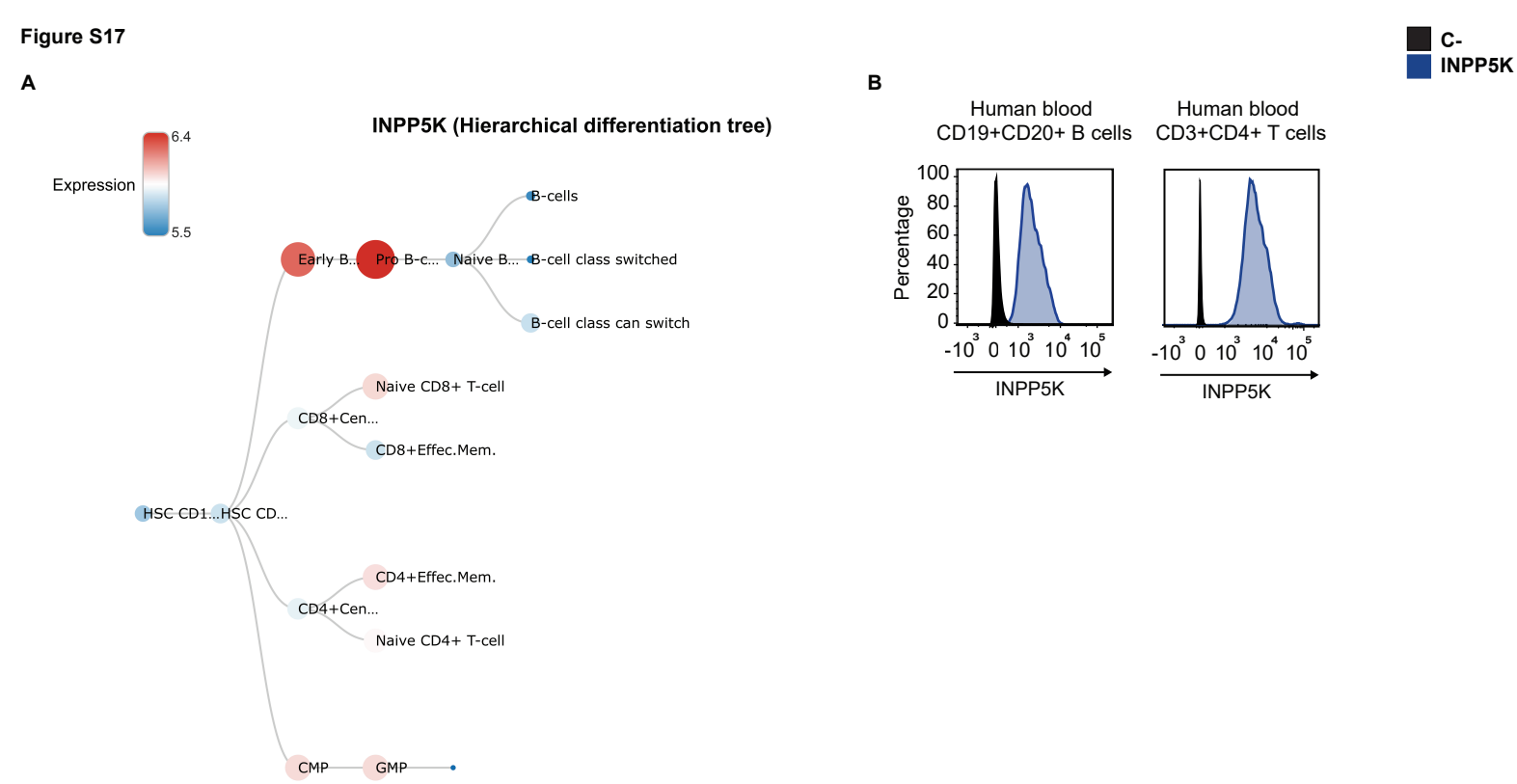
A
INPP5K (Hierarchical differentiation tree)
Expression
6.4
5.5
B-cells
Early B...
Pro B-c...
Naive B...
B-cell class switched
B-cell class can switch
Naive CD8+ T-cell
CD8+Cen...
CD8+Effec.Mem.
HSC CD1...
HSC CD...
CD4+Effec.Mem.
CD4+Cen...
Naive CD4+ T-cell
CMP
GMP
B
Human blood
CD19+CD20+ B cells
Human blood
CD3+CD4+ T cells
Percentage
100
80
60
40
20
0
-10^3 0 10^3 10^4 10^5
INPP5K
C-
INPP5K

**Figure S18**

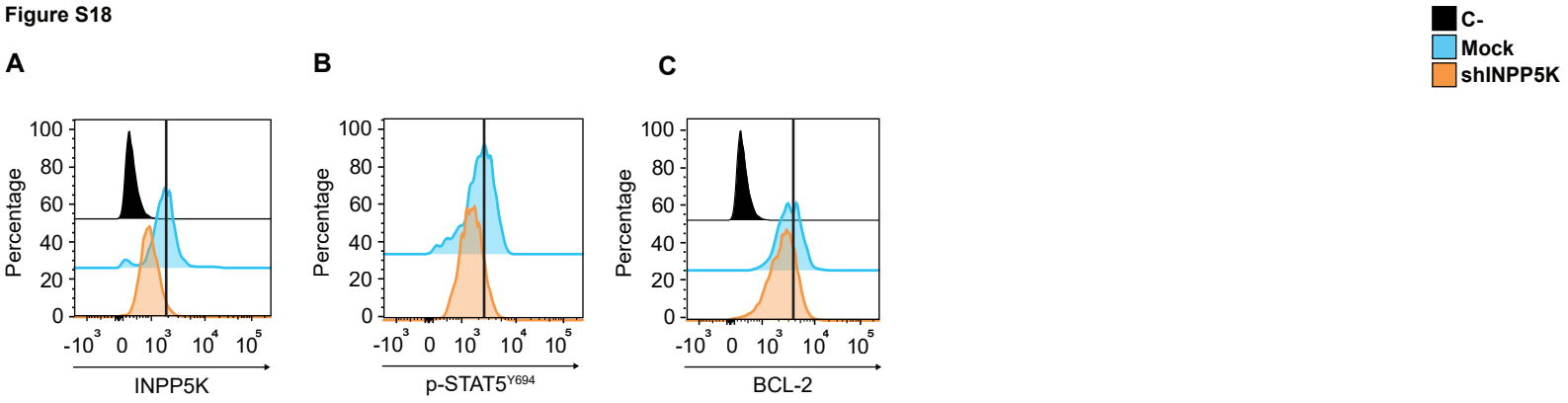
A
B
C
C-
Mock
shINPP5K
Percentage
100
80
60
40
20
0
-10^3
0
10^3
10^4
10^5
INPP5K
p-STAT5Y694
BCL-2